Comparison between $SiMe_2$ and CMe_2 Spacers as σ-Bridges for Photoinduced Charge Transfer

Cornelis A. van Walree,[†] Martin R. Roest,[‡] Wouter Schuddeboom,[§] Leonardus W. Jenneskens,*[,†] Jan W. Verhoeven,[‡] John M. Warman,[§] Huub Kooijman,[⊥] and Anthony L. Spek[⊥]

Contribution from the Debye Institute, Department of Physical Organic Chemistry, Utrecht University, Padualaan 8, 3584 CH Utrecht, The Netherlands, Laboratory of Organic Chemistry, University of Amsterdam, Nieuwe Achtergracht 129, 1018 WS Amsterdam, The Netherlands, Radiation Chemistry Department, IRI, Delft University of Technology, Mekelweg 15, 2629 JB Delft, The Netherlands, and Bijvoet Center for Biomolecular Research, Department of Crystal and Structural Chemistry, Utrecht University, Padualaan 8, 3584 CH Utrecht, The Netherlands

Received February 20, 1996[⊗]

Abstract: The potential of dimethylsilylene and isopropylidene σ-spacers as bridges for photoinduced charge transfer (CT) in 4-cyano-4′-(dimethylamino)- and 4-cyano-4′-methoxy-substituted diphenyldimethylsilanes and 2,2-diphenylpropanes was studied. Fluorescence solvatochromism and time-resolved microwave conductivity measurements show that upon photoexcitation a charge separated state $(D^{\bullet+}\sigma A^{\bullet-})^*$ is populated in all compounds. Excited state dipole moments for a given donor−acceptor combination are, irrespective of the bridge, equal. The CT states of the silanes are however lying at lower energies, implying that the presence of silicon thermodynamically facilitates the CT process. Cyclic voltammetry data of model compounds show that this is a consequence of the lowering of the acceptor reduction potential by the silicon bridge. It was however inferred from radiative decay rates that the electronic coupling between the CT and locally excited states as well as the coupling between the ground and CT state is larger for the carbon-bridged compounds. As shown by both solution and solid state electronic spectra and radiative decay rates, the photophysics of the DσA compounds are dominated by intensity borrowing of the CT transitions from transitions localized in the Dσ and σA chromophores.

Introduction

Oligosilylenes, linear or cyclic σ-bonded silicon compounds, have received considerable attention owing to their unusual electronic and photophysical properties. They exhibit intense $\sigma-\sigma^*$ electronic transitions in the near-UV region,[1−5] intermolecular charge transfer (CT) complexes involving permethylated oligosilanes have been reported,[6,7] and in photoexcited arylsilanes intramolecular CT emission originating from a $^1(\sigma,\pi^*)$ charge transfer state has been observed.[8−12] Furthermore, rapid electron transfer between chromophores connected by silicon catenates was proposed.[13] These properties find their origin in the occurrence of σ-conjugation along the silicon backbone,[1,14,15] the presence of polarizable valence electrons,[16] low ionization potentials,[3,14] and $\sigma-\pi$ interactions.[17−19] Because of these features Zyss and co-workers[20−25] investigated the second-order nonlinear optical activity, which is strongly related to the presence of intramolecular CT interactions, of donor−acceptor substituted silanes. Although moderate second-order nonlinear optical responses were found, it remained obscure whether CT between donors and acceptors takes place in oligo- and especially monosilylene-bridged compounds. In a preliminary account we have shown that photoinduced charge separation occurs in donor−acceptor substituted diphenyldimethylsilanes after initial excitation to a locally excited D*σA or DσA* state (Figure 1).[26]

[†] Department of Physical Organic Chemistry, Utrecht University.
[‡] Laboratory of Organic Chemistry, University of Amsterdam.
[§] Radiation Chemistry Department, IRI, Delft University of Technology.
[⊥] Department of Crystal and Structural Chemistry, Utrecht University.
[⊗] Abstract published in *Advance ACS Abstracts,* August 1, 1996.

(1) Miller, R. D.; Michl, J. *Chem. Rev.* **1989**, *89*, 1359−1410.
(2) Sakurai, H. *J. Organomet. Chem.* **1980**, *200*, 261−286.
(3) Pitt, C. G.; Bursey, M. M.; Rogerson, P. F. *J. Am. Chem. Soc.* **1970**, *92*, 519−522.
(4) Brough, L. F.; West, R. *J. Am. Chem. Soc.* **1981**, *103*, 3049−3056.
(5) Sun, Y.-P.; Hamada, Y.; Huang, L.-M.; Maxka, J.; Hsiao, J.-S.; West, R.; Michl, J. *J. Am. Chem. Soc.* **1992**, *114*, 6301−6310.
(6) Traven, V. F.; West, R. *J. Am. Chem. Soc.* **1973**, *95*, 6824−6826.
(7) Sakurai, H.; Kira, M.; Uchida, T. *J. Am. Chem. Soc.* **1973**, *95*, 6826−6827.
(8) (a) Shizuka, H.; Obuchi, H.; Ishikawa, M.; Kumada, M. *J. Chem. Soc., Chem. Commun.* **1981**, 405−406. (b) Shizuka, H. *Pure Appl. Chem.* **1993**, *65*, 1635−1640.
(9) Sakurai, H.; Sugiyama, H.; Kira, M. *J. Phys. Chem.* **1990**, *94*, 1837−1842.
(10) Kira, M.; Miyazawa, T.; Sugiyama, H.; Yamaguchi, M.; Sakurai, H. *J. Am. Chem. Soc.* **1993**, *115*, 3116−3124.
(11) Horn, K. A.; Grossman, R. B.; Thorne, J. R. G.; Whitenack, A. A. *J. Am. Chem. Soc* **1989**, *111*, 4809−4821.
(12) Declercq, D.; De Schryver, F. C.; Miller, R. D. *Chem. Phys. Lett.* **1991**, *186*, 467−473.
(13) Paddon-Row, M. N.; Verhoeven, J. W. *New J. Chem.* **1991**, *15*, 107−116.
(14) West, R. *Pure Appl. Chem.* **1982**, *54*, 1041−1050.
(15) Plitt, H. S.; Downing, J. W.; Raymond, M. K.; Balaji, V.; Michl, J. *J. Chem. Soc., Faraday Trans.* **1994**, *90*, 1653−1662.
(16) Bigelow, R. W.; McGrane, K. M. *J. Polym. Sci., Part B: Polym. Phys.* **1986**, *24*, 1233−1245.
(17) Pitt, C. G.; Bock, H. *J. Chem. Soc., Chem. Commun.* **1972**, 28−29.
(18) Sakurai, H. *Pure Appl. Chem.* **1987**, *59*, 1637−1646.
(19) Pitt, C. G.; Carey, R. N.; Toren, E. C., Jr. *J. Am. Chem. Soc.* **1972**, *94*, 3806−3811.
(20) Mignani, G.; Krämer, A.; Pucetti, G.; Ledoux, I.; Soula, G.; Zyss, J.; Meyrueix, R. *Organometallics* **1990**, *9*, 2640−2643.
(21) Mignani, G.; Krämer, A.; Pucetti, G.; Ledoux, I.; Soula, G.; Zyss, J. *Mol. Eng.* **1991**, *1*, 11−21.
(22) Mignani, G.; Krämer, A.; Pucetti, G.; Ledoux, I.; Zyss, J.; Soula, G. *Organometallics* **1991**, *10*, 3656−3659.
(23) Mignani, G.; Barzoukas, M.; Zyss, J.; Soula, G.; Balegroune, F.; Grandjean, D.; Josse, D. *Organometallics* **1991**, *10*, 3660−3668.
(24) Ledoux, I. *Synth. Met.* **1993**, *54*, 123−137.
(25) Morley, J. O. *J. Chem. Soc., Faraday Trans.* **1991**, *87*, 3015−3019.

S0002-7863(96)00546-X CCC: $12.00

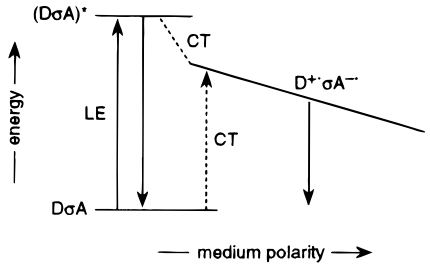

Figure 1. Schematic representation of (zero order) states in DσA compounds, showing the ground state DσA, a locally excited state (DσA)*, and the charge transfer state $D^{\bullet+}\sigma A^{\bullet-}$. The energy of the latter state is strongly dependent on the medium polarity. LE denotes a local excitation and CT a charge transfer transition.

Chart 1

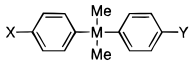

compound	M	X	Y	compound	M	X	Y
1Si	Si	Me_2N	CN	**4C**	C	MeO	H
1C	C	Me_2N	CN	**5Si**	Si	H	CN
2Si	Si	MeO	CN	**5C**	C	H	CN
2C	C	MeO	CN	**9Si**	Si	Me_2N	NMe_2
3Si	Si	Me_2N	H	**9C**	C	Me_2N	NMe_2
3C	C	Me_2N	H	**10Si**	Si	NC	CN
4Si	Si	MeO	H	**10C**	C	NC	CN

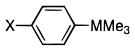

compound	M	X	compound	M	X
6Si	Si	Me_2N	**7C**	C	MeO
6C	C	Me_2N	**8Si**	Si	NC
7Si	Si	MeO	**8C**	C	NC

In the present study the potential of the $SiMe_2$ spacer as a bridge for photoinduced CT is further elaborated and its properties are compared to those of the CMe_2 bridge.[27] To this end we investigated the photophysical and electrochemical properties of 4-donor-4′-acceptor substituted diphenyldimethylsilanes and 2,2-diphenylpropanes and related compounds (Chart 1). It is shown that the charge transporting properties of the two bridges are strongly related to the interaction of these bridges with the donor and acceptor moieties, which can be traced back to the behavior of trimethylsilyl and *tert*-butyl groups as substituents. In addition, the electronic coupling between involved photophysical states is evaluated. Besides providing insight into the charge transporting capability of monoatomic bridges the present study also contributes to the understanding of photoinduced charge separation processes.

Results

Synthesis. Donor−acceptor substituted silanes **1Si** and **2Si** were prepared starting from (4-bromophenyl)chlorodimethylsilane (**11**), obtained by reaction of dichlorodimethylsilane and 4-bromophenyllithium (Scheme 1, reaction 1). Compound **11** was reacted with either 4-(dimethylamino)phenyllithium or 4-methoxyphenyllithium to give **12Si** and **13Si**, respectively. In this reaction, the use of phenyllithium instead of Grignard reagents[20] gives significantly improved yields. Finally, bromides **12Si** and **13Si** were converted into the corresponding cyanides **1Si** and **2Si** with copper(I) cyanide in DMF (reaction 9).[28] The syntheses of monosubstituted silanes **3Si**−**8Si** and *bis*substituted silanes **9Si** and **10Si** have been reported previously.[29]

4-Methoxy-substituted 2,2-diphenylpropanes **4C** and **13C** were synthesized by Friedel−Crafts alkylation of anisole with a 2-phenyl-2-propanol in the presence of either phosphoric acid or methanesulfonic acid (reaction 3).[30,31] Preparation of **4C** was conducted with phosphoric acid in 31% yield; however, use of methanesulfonic acid[32] as applied in the synthesis of **13C** gave improved results (yield 63%).

Neither a protic acid nor an aluminium chloride mediated Friedel−Crafts route was accessible for (dimethylamino)-diphenylpropanes. Therefore the synthetic pathway started with nitration of 2,2-diphenylpropane with nitronium tetrafluoroborate[33] to give 2-(4-nitrophenyl)-2-phenylpropane (**14**) (reaction 4); the *bis*nitro-substituted compound **15** was also obtained using this method. Bromination of **14** afforded **16**, while bromination of 2,2-diphenylpropane gave **17** (reaction 5). Compounds **14**, **15**, and **16** were reduced to the corresponding amines **18**, **19**, and **20**, respectively. Reduction of **14** and **15** was executed with hydrogen with palladium as catalyst. Bromide **16** was reduced with hydrazine in the presence of a ruthenium catalyst in order to circumvent dehalogenation of the bromophenyl ring.[34] Subsequently amines **18**, **19**, and **20** were methylated to their quaternary ammonium salts, which were subsequently cleaved by use of ethanolamine (reaction 7).[35] 2-(4-Bromophenyl)-2-phenylpropane (**21**) was obtained by reaction of the diazonium salt of amine **20** with hypophosporous acid (H_3PO_2) (**8**).[36] Finally, the 4-bromo-substituted diphenylpropanes **12C**, **13C**, **17**, and **21**, as well as 4-bromo-*tert*-butylbenzene, were converted into the corresponding cyanides **1C**, **2C, 10C**, **5C**, and **8C**, respectively, using copper(I) cyanide in DMF. 4-*tert*-Butylanisole (**7C**) was prepared by methylation of 4-*tert*-butylphenol with iodomethane in the presence of potassium carbonate.

Substituent Effects. In Table 1 UV absorption maxima and intensities of monosubstituted trimethylsilylbenzenes, *tert*-butylbenzenes, diphenyldimethylsilanes, and 2,2-diphenylpropanes are collected. Inspection of the data reveals that the spectra of **3**−**10Si** and **3**−**10C** are all related to the spectra of *N*,*N*-dimethylaniline, anisole, or benzonitrile. The effect of 4-positioned *tert*-butyl (tBu) and trimethylsilyl (TMS) substituents on the energy levels and electronic spectra of *N*,*N*-dimethylaniline and anisole has been discussed previously by Alt and Bock.[37] They pointed out that these substituents do

(26) van Walree, C. A.; Kooijman, H.; Spek, A. L.; Zwikker, J. W.; Jenneskens, L. W. *J. Chem. Soc., Chem. Commun.* **1995**, 35−36.

(27) Methylene-bridged donor−acceptor systems are already known to exhibit CT (intramolecular exciplex) emission. See for example: De Schryver, F. C.; Boens, N.; Put, J. *Adv. Photochem.* **1977**, *10*, 359. Okada, T.; Fujita, T.; Kubota, M.; Masaki, S.; Mataga, N.; Ide, R.; Sakata, Y.; Misumi, S. *Chem. Phys. Lett.* **1972**, *14*, 563−568. Ide, R.; Sakata, Y.; Misumi, S.; Okada, T.; Mataga, N. *J. Chem. Soc., Chem. Commun.* **1972**, 1009−1011. CT emission of a methylene-bridged donor−donor′−acceptor compound has been reported as well: Masaki, Y.; Uehara, Y.; Yanagida, S.; Pac, C. *Chem. Lett.* **1992**, 315−318.

(28) Friedman, L.; Shechter, H. *J. Org. Chem.* **1961**, *26*, 2522−2524.

(29) van Walree, C. A.; Lauteslager, X. Y.; van Wageningen, A. M. A.; Zwikker, J. W.; Jenneskens, L. W. *J. Organomet. Chem.* **1995**, *496*, 117−125.

(30) Tambotseva, V.; Tsukervanik, I. P. *J. Gen. Chem. USSR* **1945**, *15*, 820−824; *Chem. Abstr.* **1947**, *41*, 732.

(31) Tsukervanik, I. P. *J. Gen. Chem. USSR* **1945**, *15*, 699−703; *Chem. Abstr.* **1946**, *40*, 5707.

(32) Dominianni, S. J.; Ryan, C. W.; DeArmitt, C. W. *J. Org. Chem.* **1977**, *42*, 344−346.

(33) Kuhn, S. J.; Olah, G. A. *J. Am. Chem. Soc.* **1961**, *83*, 4564−4571.

(34) Mosby, W. L. *J. Org. Chem.* **1959**, *24*, 421−423.

(35) Hünig, S.; Baron, W. *Chem. Ber.* **1957**, *90*, 395−402.

(36) *Vogel's Textbook of Practical Organic Chemistry*; Longman: London, 1978; p 711.

(37) Alt, H.; Bock, H. *Tetrahedron* **1971**, *27*, 4965−4975.

Scheme 1

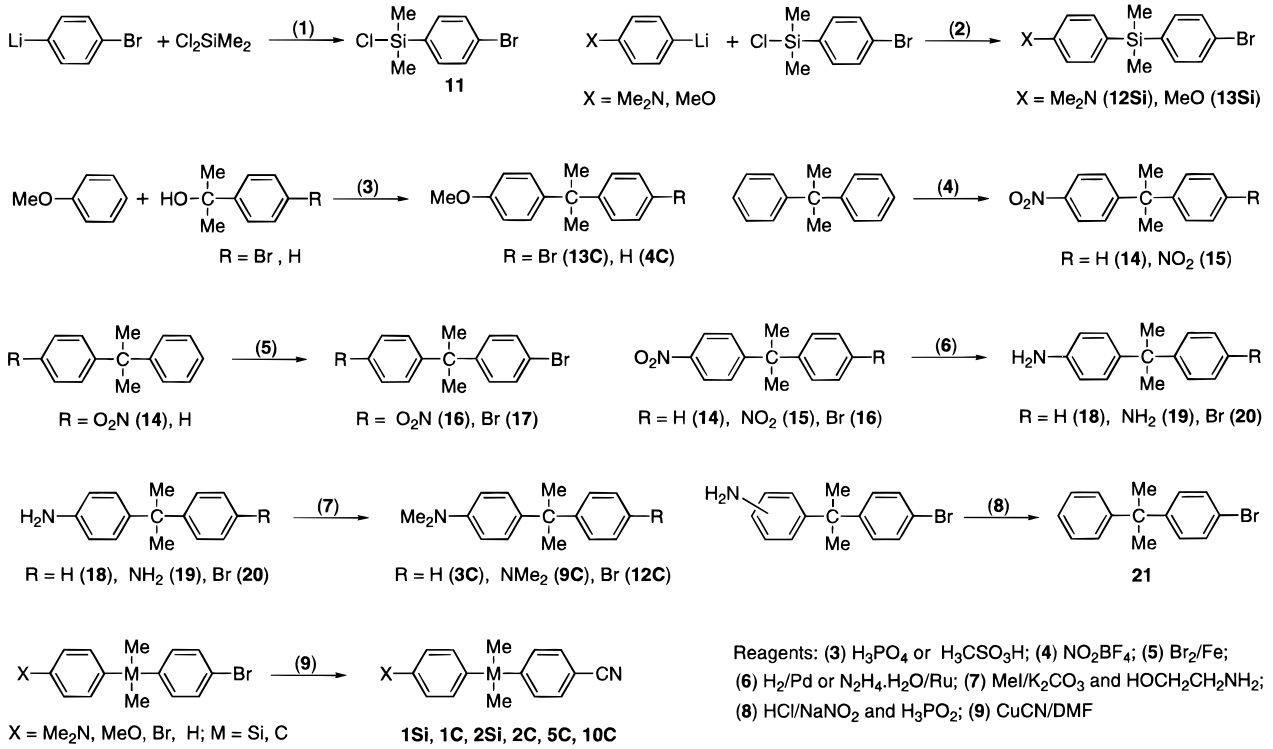

Table 1. UV and Fluorescence Data, in Cyclohexane, of Donor or Acceptor Substituted Diphenyldimethylsilanes, 2,2-Diphenylpropanes, Trimethylsilylbenzenes, *tert*-Butylbenzenes, and Benzenes

	^1L_a		^1L_b		fluorescence	
compd	ν_{max}[a]	ϵ_{max}[b]	ν_{max}[a]	ϵ_{max}[b]	ν_{fl}[a]	Φ_{fl}[c]
3Si	37.3	27.7	32.8	sh	29.9	0.13
3C	39.1	19.2	33.0	2.4	29.8	0.24
4Si	43.5	7.9	*36.5*/35.6[d]	0.70	33.2	0.09
4C	44.2	13.2	*36.1*/35.2[d]	2.1	33.3	0.41
5Si	*42.4*/41.3[d]	20.1	*36.5*/35.5[d]	1.0	33.7/32.9	0.28
5C	42.4	15.9	*37.3*/35.8[d]	0.95	34.1/33.1	0.26
6Si	37.9	26.6	33.6	sh	30.2	0.20
6C	39.7	14.5	33.1	2.1	30.0	0.19
7Si	43.5	12.1	*36.5*/35.7[d]	1.4	33.3	0.19
7C	44.8	10.3	*36.2*/35.5[d]	2.0	33.6	0.48
8Si	*42.9*/41.7[d]	17.9	36.6/*35.5*[d]	0.80	33.8/33.0	0.33
8C	*43.5*/42.0[d]	15.9	*37.6*/36.1[d]	0.50	34.1/33.3	0.18
9Si	37.0	44.6	33.6	sh	30.2	0.22
9C	38.6	35.6	33.1	4.8	29.9	0.19
10Si	42.4/*41.3*[d]	54.5	*36.4*/35.3[d]	1.8	33.7/32.9	0.43
10C	*42.4*/41.3[d]	28.8	*37.3*/35.8[d]	1.1	34.1/33.3	0.22
$C_6H_5NMe_2$	39.8	14.9	33.6	2.3	30.3	0.19
C_6H_5OMe	45.5	7.8	*36.9*/36.0[d]	2.1	34.0	0.45
C_6H_5CN	*45.2*/43.5[d]	12.0	*37.0*/36.2[d]	0.62	34.6/33.9	0.23

[a] Units 10^3 cm^{-1}. [b] Units 10^3 M^{-1} cm^{-1}. [c] Fluorescence quantum yield. [d] Main vibrational components; the ϵ_{max} value refers to the most intensive component given in italics.

not affect the SHOMO (HOMO-1) and LUMO owing to their nodal character at the 1 and 4 positions (Figure 2). The HOMO energies of *N*,*N*-dimethylaniline and anisole are slightly raised by the inductively donating tBu substituent. The TMS group is inductively donating as well, but this effect is opposed by its mesomeric electron accepting behavior,[19,25,37−39] so that the net perturbation of the HOMO should be small. These substituent effects are more or less in line with cyclic voltammetry data, which reveal that **6C** has a comparable oxidation potential as *N*,*N*-dimethylaniline, whereas the potential of **6Si** is somewhat more positive (Table 2). The latter observation suggests that the electron accepting effect of the TMS group is somewhat stronger than the electron donating effect. In contrast, the oxidation potential of anisole seems to be hardly affected by the TMS substituent, whereas for **7C** the potential is reduced by some 0.2 V. However, owing to the irreversible nature of the electrode process electrochemical oxidation potentials of anisoles do not adequately reflect their ionization potentials.[40]

The ^1L_b bands of anilines and anisoles correspond predominantly to a HOMO-LUMO transition. Consequently, they are not shifted significantly by tBu and TMS substitution,[37] as the orbitals involved are either not (LUMO) or only slightly (HOMO) affected by substitution. The tBu group, being an inductive donor, raises both the HOMO and SLUMO, in about equal amounts.[41] The ^1L_a bands of **6C** and **7C**, which are predominantly based on promotion of an electron from the HOMO to the SLUMO, are therefore hardly shifted with respect to those of *N*,*N*-dimethylaniline and anisole. The ^1L_a bands are however substantially affected by the TMS group. The HOMO was seen to be only weakly sensitive to this group, but the TMS substituent substantially lowers the energy of the SLUMO, presumably as a result of (p−d)π bonding.[19,37,42] This results in a bathochromic shift of *ca.* 2000 cm^{-1} for the ^1L_a transitions, which can be regarded as involving CT from the dimethylamino toward the TMS moiety. The shift of the ^1L_a band is more pronounced for **6Si** than for **7Si** because the CT character of the transition is larger for the stronger donating dimethylamino group.[37]

The SLUMO and SHOMO of benzonitrile are insensitive to substitution, again as a consequence of nodes at the 1 and 4 positions. The tBu group raises the energy of both the HOMO

(38) Bock, H.; Seidl, H.; Fochler, M. *Chem. Ber.* **1968**, *101*, 2815−2822.
(39) Bock, H.; Alt, H. *J. Am. Chem. Soc.* **1970**, *92*, 1569−1570 and references cited.
(40) Zweig, A.; Hodgson, W. G.; Jura, W. H. *J. Am. Chem. Soc.* **1964**, *86*, 4124−4129.
(41) Jaffé, H. H.; Orchin, M. *Theory and Applications of Ultraviolet Spectroscopy*; Wiley: New York, 1962.
(42) Weeks, G. H.; Adcock, W.; Klingensmith, K. A.; Waluk, J. W.; West, R.; Vasak, M.; Downing, J.; Michl, J. *Pure Appl. Chem.* **1986**, *58*, 39−53.

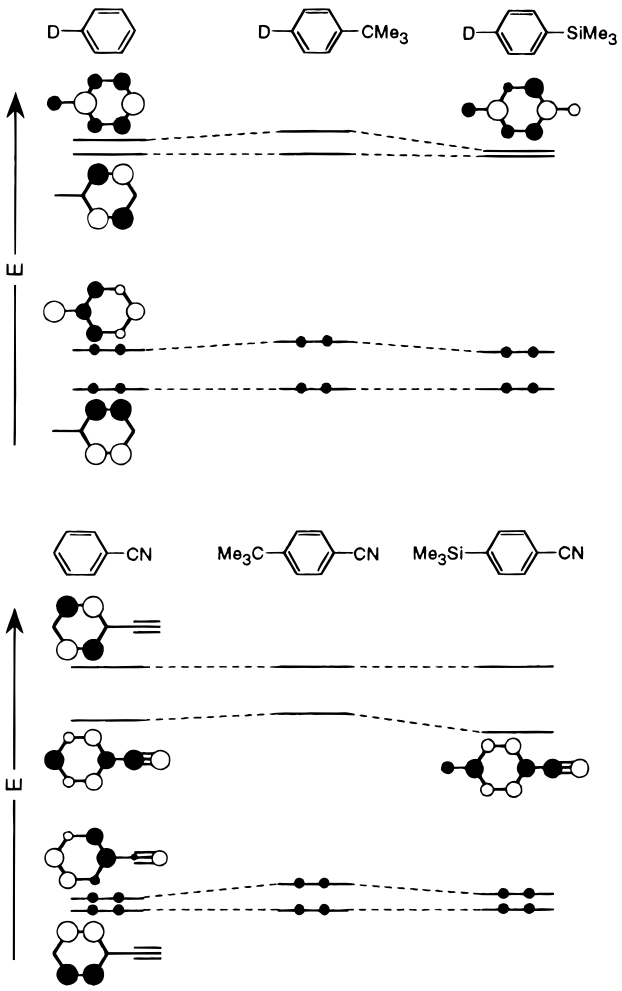

Figure 2. Qualitative MO diagram of donor benzenes (D = Me_2N, MeO) and benzonitrile and their 4-*tert*-butyl- and 4-trimethylsilyl substituted derivatives. Orbital coefficients were obtained from extended Hückel calculations (see Experimental Section).

Table 2. Cyclic Voltammetry Data of Donor or Acceptor Substituted Diphenyldimethylsilanes, 2,2-Diphenylpropanes, Trimethylsilylbenzenes, *tert*-Butylbenzenes, and Benzenes[a]

compd	E_{ox}	E_{red}	compd	E_{ox}	E_{red}
1Si	+0.79	−2.30	**5Si**		−2.28
1C	+0.70	−2.51	**5C**		−2.52
2Si	+1.75	−2.29	**6Si**	+0.71	
2C	+1.75	−2.52	**6C**	+0.63	
3Si	+0.74		**7Si**	+1.74	
3C	+0.69		**7C**	+1.52	
4Si	+1.78		**8Si**		−2.34
4C	+1.57		**8C**		−2.56
$C_6H_5NMe_2$	+0.64		C_6H_5CN		−2.46
C_6H_5OMe	+1.74				

[a] Halve-wave oxidation (E_{ox}) and reduction potentials (E_{red}) are given in V relative to SCE.

and LUMO, while the TMS group hardly affects the HOMO energy and stabilizes the LUMO. The cyclic voltammetry data show that the reduction potential of **8Si** is 0.12 V lower than that of benzonitrile and 0.22 V lower than that of **8C**. The ^1L_a band, mainly associated with the HOMO-LUMO transition,[43] is shifted by introduction of both the tBu and TMS groups. In the case of **8C** this shift is caused by an increase of the HOMO energy, while in the case of **8Si** the lowering of the LUMO is responsible. The shift of the benzonitrile ^1L_b band upon substitution is small.

(43) Del Bene, J.; Jaffé, H. H. *J. Chem. Phys.* **1968**, *49*, 1221−1229.

Oxidation potentials of donor substituted diphenyldimethylsilanes **3Si** and **4Si** and 2,2-diphenylpropanes **3C** and **4C** all are slightly more positive than those of analogously substituted (trimethylsilyl)- and *tert*-butylbenzenes. Replacement of a methyl group of the $SiMe_3$ and CMe_3 groups by a phenyl group apparently leads to a somewhat modified substituent behavior. The lowering of the cyanophenyl reduction potential by the dimethylphenylsilyl substituent of **5Si** is stronger than that by the TMS group of **8Si**. The reduction potential of **5C**, on the other hand, is higher than that of **8C**. Consequently, a difference of 0.22 eV is found between the reduction potentials of **8Si** and **8C**.

Despite the changes in redox potentials the UV spectra of the monosubstituted diphenyldimethylsilanes and diphenylpropanes hardly differ from the corresponding (trimethylsilyl)- and *tert*-butylbenzenes. Generally, the positions of ^1L_b bands are not shifted, while shifts of the ^1L_a bands are small, *ca.* 600 cm^{-1}. It can thus be concluded that excitations are localized in the anilino, anisyl, and cyanophenyl moieties. The *bis*substituted compounds **9Si**, **9C**, **10Si**, and **10C** display the same UV maxima as their analogues of type **3** and **5** as well. Hence, no substantial electronic interaction between two donors or acceptors across silicon and carbon can be inferred. Intensities of the ^1L_a and ^1L_b bands of the *bis*substituted compounds are to a first approximation twice as large as those of the compounds containing only one dimethylamino or cyano group, reflecting the presence of two identical chromophores in one molecule.

Fluorescence emission maxima and quantum yields are also recorded in Table 1. For a given donor hardly any shift in emission maximum upon substitution is observed whereas distinct differences were found in the UV spectra. Consequently, the type of donor determines the emission wavelength; in the lowest singlet excited state the silicon or carbon containing substituent is not contributing. This compares favorably with the nature of the lowest lying (^1L_b) excited state as the position of the LUMO is independent of substituents (Figure 2). This also rationalizes that for donor substituted compounds differences in fluorescence maxima between compounds containing $SiMe_3$ and $SiMe_2C_6H_5$ groups or CMe_3 and $CMe_2C_6H_5$ groups, respectively, are marginal. For the cyanides a small difference of some 400 cm^{-1} between the emission maxima of the carbon and silicon based substituents is observed; the latter are situated at lower energies. Moreover, there is a clear bathochromic shift with respect to benzonitrile. Fluorescence quantum yields of the donor substituted silicon containing compounds **3Si**, **4Si**, **6Si**, and **7Si** are generally lower than or equal to the values of their analogues with carbon-based substituents. For the cyanides quantum yields of the silanes are generally higher.

Donor−Acceptor Substituted Compounds. The UV spectra (Figure 3) of the donor−acceptor substituted compounds **1Si**, **2Si**, **1C**, and **2C** are composed of the transitions appearing in reference compounds containing only a donor or acceptor chromophore (*e.g.* **3Si** and **5Si** for **1Si**). It is however seen in Figure 3 that enhanced absorption occurs below 35 000 cm^{-1},[44] which arises from a transition involving the anilino or anisyl donor and cyanophenyl acceptor orbitals and can be designated as a CT absorption. No concentration dependence on the UV spectra was observed, implying that the CT is intramolecular in nature. The presence of discrete intramolecular CT bands

(44) Difference spectroscopy revealed that the CT bands of both **1Si** and **1C** are situated at 34 800 cm^{-1}, while those of **2Si** and **2C** are difficult to determine reliably. According to the relation $\nu_{CT} = E_{ox}(D) - E_{red}(A) + C$ (compare with eq 3) the CT bands of the silanes should be red shifted to the CT bands of the diphenylpropanes. This discrepancy is in line with an earlier report (ref 47) on the unreliability of determining CT maxima by difference spectroscopy.

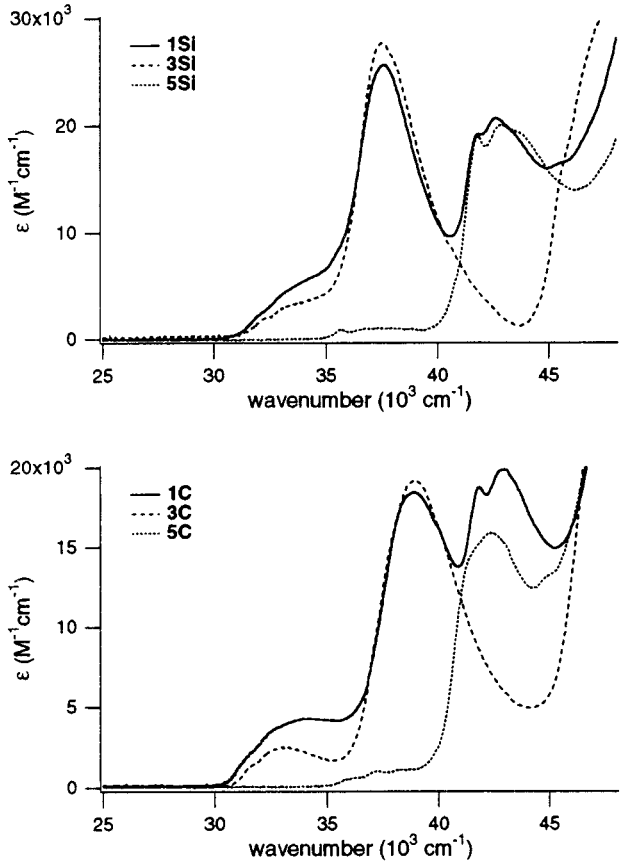

Figure 3. UV spectra in cyclohexane of donor−acceptor compounds **1Si** (top) and **1C** (bottom) and their separate chromophores.

Table 3. UV Transitions of Donor−Acceptor Substituted Diphenyldimethylsilanes and 2,2-Diphenylpropanes in Cyclohexane

	^1L_a		^1L_b	
compd	ν_{max}[a]	ϵ_{max}[b]	ν_{max}[a]	ϵ_{max}[b]
1Si	37.6[c]/42.7[d]	25.7[c]/19.0[d]	*e*	*e*
1C	38.9[c]/42.9[d]	18.4[c]/20.3[d]	*e*	*e*
2Si	42.9[f]	18.8	*36.5*/35.6[f]	2.0
2C	44.2[f]	23.2	35.1[f]	2.4

[a] Units 10^3 cm^{-1}. [b] Units 10^3 M^{-1} cm^{-1}. [c] Donor band. [d] Acceptor band. [e] Submerged under other bands. [f] Superposition of donor and acceptor bands.

indicates that a ground state donor−acceptor interaction exists and that a charge separated state $D^{\bullet+}\sigma A^{\bullet-}$ can be populated directly from the ground state.

As the intensity of the ^1L_a transitions in the spectra of the donor−acceptor compounds is lower than the summation of the ^1L_a transitions of the model compounds, it appears that the CT transitions borrow intensity from the donor and acceptor ^1L_a transitions. *I.e.*, mixing of the CT state with locally excited ^1L_a states ($D^*\sigma A$ and $D\sigma A^*$) occurs.[45−47] Furthermore, the small but distinct hypsochromic shift of the ^1L_a bands of the donor−acceptor substituted compounds (Table 3) with respect to the ^1L_a maxima of the reference compounds suggests that the local transitions mix with the CT transition *via* configuration interaction.[46] A hypsochromic shift for the ^1L_a bands of methoxy compounds **2Si** and **2C** is not revealed by the data in Table 3 because overlapping of bands obscures the actual maxima. The ^1L_b bands are not involved in the CT process because of the presence of nodes at the substitution positions of the orbitals involved in these transitions.

The oxidation and reduction potentials of the donor−acceptor substituted compounds (Table 2) are generally within experimental error equal to those of the separate chromophores. The only redox potential which deviates from that of its separate chromophores is the oxidation potential of **2C**. As already discussed above the oxidation potentials of the methoxy compounds are not too reliable. Ground state interactions can thus not be inferred from the cyclic voltammetry data.[48]

Fluorescence spectra of **1C**, **2C**, **1Si**, and **2Si** are highly dependent on the solvent polarity (Table 4). The bathochromic shift with increasing solvent polarity is typical of CT fluorescence originating from a charge separated state $D^{\bullet+}\sigma A^{\bullet-}$. The spectra of all compounds consist of a single emission band in all solvents, excepted **1Si** in acetonitrile where the CT emission is so weak that another band centered at 25 640 cm^{-1} becomes visible. This is probably a local emission. Time resolved fluorescence measurements showed that the two emission bands behave independently, indicating that they are related to separate photophysical phenomena.

A quantitative relationship between the CT fluorescence maxima and the solvent polarity is provided by the Lippert−Mataga equation:[49]

$$\nu_{CT} = \nu_{CT}(0) - \frac{2\mu_e^2}{hc\rho^3}\Delta f \qquad (1a)$$

with

$$\Delta f = \frac{\epsilon_s - 1}{2\epsilon_s + 1} - \frac{n^2 - 1}{4n^2 + 2} \qquad (1b)$$

where ν_{CT} denotes the emission wavenumber, $\nu_{CT}(0)$ the (hypothetical) gas-phase emission wavenumber, μ_e the excited state dipole moment (the ground state dipole moment is neglected in eq 1a), *h* the Planck constant, *c* the light velocity, and ρ the Onsager radius of the solute. The solvent polarity parameter Δf is related to the solvent dielectric constant ϵ_s and refractive index *n* (eq 1b).[50] Plotting of ν_{CT} *vs* Δf enables the calculation of the excited state dipole moment μ_e from the slope of the linear fit, provided that the Onsager radius ρ of the solute is known.

The solvatochromic relationships are shown in Figure 4, and parameters of these relationships are given in Table 4. For all compounds a satisfactory linear relationship is found. However, the solvatochromic behavior of **2C** is more appropriately described by two relationships, one for solvents of low polarity and one for solvents of high polarity, suggesting that as a function of solvent polarity different emitting species are present. This can be rationalized by taking the driving force ΔG^0 for photoinduced CT processes into account, which is given by:[51]

$$\Delta G^0 = E_{ox}(D) - E_{red}(A) - E_{00} + C \qquad (2a)$$

with

(45) Murrell, J. N. *The Theory of the Electronic Spectra of Organic Molecules*; Methuen: London, 1963; p 271.
(46) Pasman, P.; Rob, F.; Verhoeven, J. W. *J. Am. Chem. Soc.* **1982**, *104*, 5127−5133.
(47) Verhoeven, J. W.; Dirkx, I. P.; de Boer, T. J. *Tetrahedron* **1969**, *25*, 4037−4055.
(48) Fourmigué, M.; Huang, Y.-S. *Organometallics* **1993**, *12*, 797−802.
(49) Beens, H.; Knibbe, H.; Weller, A. *J. Chem. Phys.* **1967**, *47*, 1183−1184.
(50) Solvent dielectric constants and refractive indices were taken from the following: Reichardt, C. *Solvents and Solvent Effects in Organic Chemistry*, 2nd ed.; VCH: Weinheim, 1988.
(51) Weller, A. *Z. Phys. Chem.* **1982**, *133*, 93−98.

Table 4. Fluorescence Emission Maxima (ν_{CT}) and Quantum Yields (Φ_{fl}) of Dimethylsilylene- and Isopropylidene-Bridged Donor−Acceptor Compounds in Various Solvents and Results of Solvatochromic Fits

		1Si		**2Si**		**1C**		**2C**	
solvent	Δf	ν_{ct}[a]	Φ_{fl}	ν_{ct}[a]	Φ_{fl}	ν_{ct}[a]	Φ_{fl}	ν_{ct}[a]	Φ_{fl}
cyclohexane	0.100	28.17	0.04	33.67[b]	0.11	29.76	0.22	33.35	0.48
benzene	0.115	23.31[b,c]	0.12			25.00[b]	0.15		
pentyl ether	0.173	23.39	*d*	30.12	*d*	25.64	*d*	32.05	*d*
butyl ether	0.193	23.98	*d*	29.76	*d*	26.00	*d*	32.26	*d*
diethyl ether	0.251	22.60	0.10	28.17	0.04	24.39	0.24	31.09	0.58
ethyl acetate	0.292	19.81	0.08	26.30	0.05	21.60	0.37	27.93	0.25
THF	0.308	19.77	0.07	26.21	0.04	21.65	0.44	27.78	0.26
butyronitrile	0.376	17.67	*d*	24.36	*d*	19.42	*d*	26.39	*d*
acetonitrile	0.392	16.67[e]	0.0015	23.27	0.13	18.28	0.03	25.00	0.31
$-2\mu_e^2/hc\rho^3$ [a]		36.51		30.78		37.18		26.50[f]	14.51[g]
$\nu_{ct(0)}$[a]		31.03		35.61		33.03		35.84[f]	34.79[g]
corr coeff		0.983		0.995		0.989		0.954[f]	0.975[g]

[a] Units 10^3 cm^{-1}. [b] Not used in solvatochromic fit. [c] Excitation wavenumber 35 090 cm^{-1}. [d] Not determined because of solvent absorption at 37 740 cm^{-1}. Excitation wavenumber 33 330 cm^{-1} for **1Si** and **1C** and 35 090 cm^{-1} for **2Si** and **2C**, respectively. [e] Another band observed at 25 640 cm^{-1}. [f] Polar solvents. [g] Nonpolar solvents.

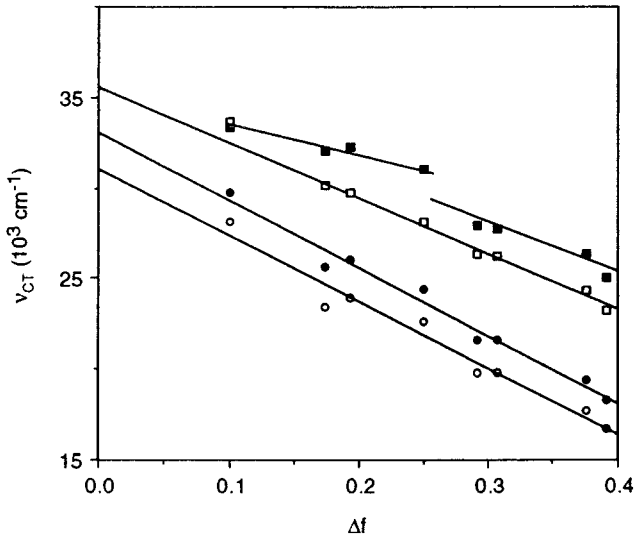

Figure 4. Fluorescence solvatochromism of donor−acceptor substituted compounds **1Si** (open circles), **1C** (filled circles), **2Si** (open squares), and **2C** (filled squares).

$$C = -\frac{e^2}{\epsilon_s R_{DA}} - \left(\frac{e^2}{2}\right)\left(\frac{1}{r_{D^+}} + \frac{1}{r_{A^-}}\right)\left(\frac{1}{35.9} - \frac{1}{\epsilon_s}\right) \qquad (2b)$$

In these equations E_{00} represents the zero−zero excitation energy, e the elementary charge, R_{DA} the donor−acceptor center-to-center distance, and r_{D^+} and r_{A^-} the effective radii of the radical cations and anions, respectively. E_{ox}(D) is the oxidation potential of the donor and E_{red}(A) the reduction potential of the acceptor as measured in acetonitrile ($\epsilon_s = 35.9$); the term C corrects for the solvent effect by taking into account the Coulombic attraction energy between radical cations and anions and a solvation free energy term. Equations 2a and 2b can be conveniently combined to

$$\Delta G^0 = \Delta G^0_\infty - K_1 + K_2/\epsilon_s \qquad (2c)$$

in which $\Delta G^0_\infty = E_{ox}(D) - E_{red}(A) - E_{00}$[52] ($\epsilon_s$ being infinitely large) and K_1 and K_2 constants are determined by the type of bridge *via* R_{da}, r_{D^+}, and r_{A^-}. R_{DA} was taken as the distance between the centers of the aromatic rings in the crystal structure of **1Si** for the silanes (R_{DA} = 5.4 Å) and **1C** for the diphenylpropanes (R_{DA} = 4.9 Å). The effective radii r_{D^+} and r_{A^-} were estimated from the molecular volumes V_m of **1Si** (392 Å^3) and **1C** (364 Å^3) in their crystal structures by $r_{D^+} = r_{A^-} = (3V_m/4\pi)^{1/3}$, giving 4.5 Å for **1Si** and **2Si** and 4.4 Å for **1C** and **2C**. K_1 and K_2 values obtained with these parameters are collected in Table 5.

(52) The redox potentials of the reference chromophores (**3Si**, **5Si**, and so on) were used to obtain ΔG^0_∞. However, for the uncertain oxidation potential of **2C** the value of the compound itself, +1.75 V, was used.

Table 5. Thermodynamic Data for Photoinduced Charge Transfer in Donor−Acceptor Compounds

compd	E_{00}[a] (eV)	ΔG^0_∞[b] (eV)	K_1[b] (eV)	K_2[b] (eV)	$\epsilon_{s(0)}$[b]	ΔG^0_{chx}[c] (eV)
1Si	3.71	−0.69	0.09	0.53	0.7	−0.52
1C	3.76	−0.55	0.09	0.31	0.5	−0.49
2Si	4.19	−0.13	0.09	0.53	2.4	+0.04
2C	4.25	+0.02	0.09	0.31	4.4	+0.08

[a] Zero−zero transition energy, taken as the onset of the UV spectrum. [b] See text for explanation. [c] Driving force in cyclohexane (ϵ_s = 2.015).

Equation 2c implies that upon going to a less polar solvent ΔG^0 becomes more positive; at a certain medium polarity CT is thermodynamically not allowed anymore. The dielectric constants at which ΔG^0 is zero, $\epsilon_s(0)$, and the driving force in cyclohexane (ϵ_s = 2.015) are given in Table 5. These data show that in the dimethylamino compounds **1Si** and **1C** photoinduced CT is feasible even in cyclohexane, the most nonpolar solvent. In contrast, CT is forbidden for **2C** in solvents with $\epsilon_s < 4.4$. This result corresponds nicely to the data shown in Figure 4, which reveal that in diethyl ether (ϵ_s = 4.2) and solvents of lower polarity another emitting species is present than in high-polarity solvents. Since the emission in the low-polarity solvents is still moderately solvatochromic, it is anticipated that a partially charge separated state $D^{\delta\bullet+}\sigma A^{\delta\bullet-}$ is present. The $\epsilon_s(0)$ value for **2Si**, 2.4, indicates that this is also the case for this compound in cyclohexane. Indeed the emission maximum for **2Si** in cyclohexane deviates from the solvatochromic fit and coincides with the emission maxima of its separate chromophores **4Si** and **5Si**.[26]

Excited state dipole moments μ_e were obtained from the slopes of the solvatochromic fits (eq 1a). Radii ρ were estimated by $\rho = (3V_m/4\pi)^{1/3}$, giving 4.5 Å for the diphenyldimethylsilanes and 4.4 Å for the diphenylpropanes (*vide supra*). With these values excited state dipole moments of 18.2 (**1Si**), 17.7 (**1C**), 16.7 (**2Si**), 15.0 (**2C**, polar solvents), and 11.1 D (**2C**, nonpolar solvents), respectively, were obtained. The μ_e obtained for **2C** in polar solvents seems to be rather small in comparison with the excited state dipole moment of the other compounds, but inspection of Figure 4 reveals that this is caused by a somewhat

deviating emission maximum in butyronitrile. With the exception of the value for **2C** in nonpolar solvents, the dipole moments correspond to a unit charge separation over 3.1−3.8 Å. Since the distance between the centers of the anilino or anisyl and cyanophenyl moieties is estimated from X-ray structures to be 5.4 Å for the silanes and 4.9 Å for the carbon compounds, 63−70% of an elementary charge is transferred over the donor−acceptor distance. Although this suggests at first sight that full CT does not take place, obtained μ_e values are very sensitive to the magnitude of ρ. In view of the uncertainty in both ρ and the donor−acceptor distance it is therefore difficult to decide whether full or partial CT occurs.

Excited state dipole moments are thus virtually independent of the bridge and are determined by the donor−acceptor combination only. For a given donor−acceptor combination the almost parallel solvatochromic plots show that the energies of the CT states of the silicon-bridged compounds are a systematic amount lower than those of their carbon-bridged counterparts. This is understood by considering the solvent dependence of the CT state energies E_{CT}, given by[53]

$$E_{CT} = E_{ox}(D) - E_{red}(A) + C' - \mu_e^2 \frac{2}{\rho^3} \frac{\epsilon_s - 1}{2\epsilon_s + 1} \qquad (3)$$

Taking μ_e, ρ, and the Coulomb term C' equal for a given donor−acceptor pair, differences in E_{CT} appear to be determined only by differences in oxidation and reduction potentials. This applies nicely to the dimethylsilylene- and isopropylidene-bridged donor−acceptor compounds. The difference in $E_{ox}(D) - E_{red}(A)$ for the pair **1Si** and **1C** is 0.19 eV; for **2Si** and **2C** the value is 0.21 eV (Table 2). The emission wavenumber of **1Si** is on average 0.23 eV (1820 cm^{-1}) lower than that of **1C**, while the emission energy difference between **2Si** and **2C** is on average 0.22 eV (1740 cm^{-1}) in the polar solvents. Consequently, a dimethylsilylene bridge provides an energetically more favorable pathway for CT to occur than a isopropylidene bridge by relatively lowering the CT state by some 0.2 eV. Full CT probably occurs for instance in **2Si** in etheral solvents, whereas only partial CT is observed in its analogue **2C** in these solvents. As was seen above the 0.2-eV difference is predominantly caused by a lowering of the cyanophenyl acceptor reduction potential by the dimethylsilylene bridge.

Time-Resolved Microwave Conductivity Studies. The nature of the excited state of **1Si** and **1C** was further elucidated using the flash-photolysis time-resolved microwave conductivity (TRMC) technique.[54−56] The formation of dipolar excited states upon pulsed laser photoexcitation (flash-photolysis) leads to an increase in the high-frequency dielectric loss of a solution. Using the TRMC technique this increase is monitored by time-resolved measurement of the change in microwave conductivity $\Delta\sigma$ which is related to the difference in dipole moment of the excited state μ_e and ground state μ_g according to:

$$\Delta\sigma = (\epsilon_s + 2)^2 N(\mu_e^2 - \mu_g^2) F_{\omega\Theta}/27 k_B T\Theta \qquad (4)$$

with N being the solute concentration, k_b the Boltzmann constant, T the temperature, and $F_{\omega\Theta}$ a factor containing the applied microwave frequency ω and the dipole relaxation time Θ: $F_{\omega\Theta} = (\omega\Theta)^2/[1 + (\omega\Theta)^2]$. The dipole relaxation time Θ, *i.e.* the mean time required for randomization of the dipole orientation, depends on the solute geometry and the solvent viscosity.

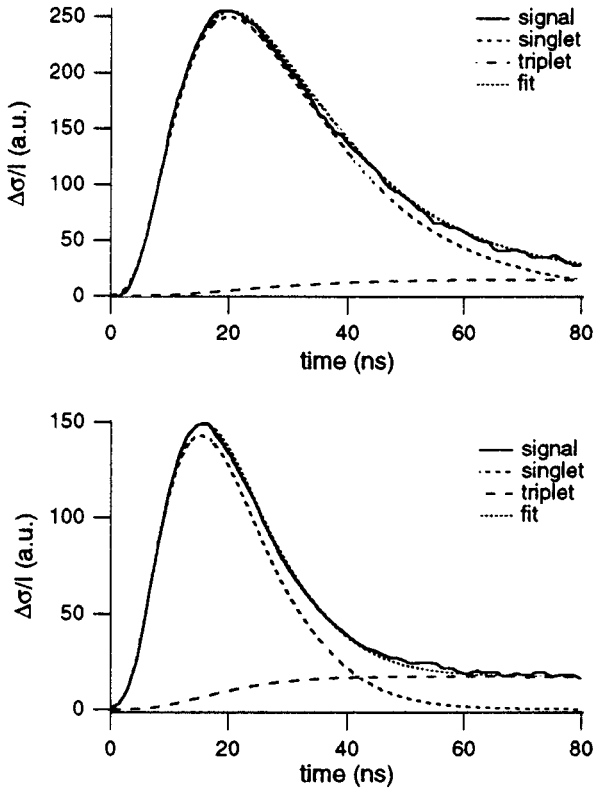

Figure 5. Time-resolved microwave conductivity transients of **1Si** (top) and **1C** (bottom) in benzene. Apart from the measured signals the singlet and triplet components of the fits to the experimental data are shown.

TRMC transients of **1Si** and **1C** in benzene are shown in Figure 5. In both cases, an initial short-lived component with a lifetime of 18 ns for **1Si** and 7 ns for **1C**, followed by a long-lived (hundreds of nanoseconds) component, is discernible. These components are attributed to the singlet and triplet excited states, respectively. Both excited states possess a dipole moment substantially larger than that of the ground state, confirming the formation of charge separated states. It is conspicuous that the triplet state contribution to the TRMC transient is larger for **1C** than for **1Si**. On the basis of the heavy atom effect[57] the opposite behavior would have been expected. The larger triplet component found for **1C** may be related to the occurrence of exciton coupling between the two phenyl moieties, which is known to be present in diphenylmethanes and related compounds and favors intersystem crossing.[58] Owing to their closer proximity, the degree of exciton coupling between the phenyl moieties will be larger for **1C**.

Excited state dipole moments can be derived from the absolute magnitude of the TRMC transients if the dipole relaxation time is known. For the present molecules Θ may be taken to be controlled by rotational diffusion of the molecules and therefore can be equated with the rotational diffusion time, Θ_R. A method for calculating Θ_R for molecules with spherical, cylinder-like and disk-like geometries has been described.[56] Since the geometries of **1Si** and **1C** are intermediate between that of a sphere and that of a cylinder, we have calculated Θ_R for these two extremes. This results in 70 ps < Θ_R < 189 ps for **1Si** and 66 ps < Θ_R < 165 ps for **1C**. Using these limiting

(53) Rettig, W. *Angew. Chem.* **1986**, *98*, 969−986.
(54) de Haas, M. P.; Warman, J. M. *Chem. Phys.* **1982**, *73*, 35−53.
(55) Infelta, P. P.; de Haas, M. P.; Warman, J. M. *Radiat. Phys. Chem.* **1980**, *15*, 273.
(56) Schuddeboom, W. Ph.D. Thesis, Delft University of Technology, 1994.
(57) Turro, N. J. *Modern Molecular Photochemistry*; Benjamin/Cummings: Menlo Park, 1978; p 125.
(58) Kasha, M.; Rawls, H. R.; El-Bayoumi, M. A. *Pure Appl. Chem.* **1965**, *11*, 371−392.

Table 6. Solvent Dependence of Fluorescence Lifetimes and Radiative Decay Rates

	1Si			**1C**		
solvent	τ_{fl}[a]	k_{rad}[b]	g^*	τ_{fl}[a]	k_{rad}[b]	g^*
cyclohexane	1.7	23.5	0.058	2.8	78.6	0.19
benzene	18[c]	6.7	0.025	7[c]	21.4	0.084
diethyl ether	19.6	5.1	0.022	8.4	28.5	0.077
ethyl acetate	29.6	2.7	0.016	34.0	10.9	0.055
acetonitrile	1.8	0.83	0.011	5.0	6.0	0.038

[a] Units ns. [b] Units 10^6 s^{-1}. [c] Lifetime obtained with TRMC experiment.

values of Θ together with PM3 calculated ground state dipole moments of 5.0 (**1Si**) and 4.1 D (**1C**) results in estimates of the excited state dipole moments within the range 16 D $< \mu_e <$ 25 D and 15 D $< \mu_e <$ 23 D for **1Si** and **1C**, respectively. The actual dipole moments would be expected to lie close to the means of these extremes, *i.e.* 20.5 and 19 D. The values of 18.2 and 17.7 D determined from solvatochromic shifts are seen to be in reasonably good agreement with these estimates from the TRMC results.

Radiative Decay Rates and Interstate Electronic Couplings. Fluorescence quantum yields of the donor−acceptor compounds display a general trend of maximizing at medium solvent polarity (Table 4). Often a monotonous decrease with increasing medium polarity is found for donor−acceptor systems. The trend in quantum yields found here has been explained previously by the occurrence of intersystem crossing to locally excited triplet states in nonpolar solvents.[59] Fluorescence lifetimes τ_{fl} of **1Si** and **1C**, presented in Table 6, follow a similar trend as the quantum yields: they reach a maximum at medium solvent polarity (ethyl acetate). It is conspicuous that lifetimes are quite long for compounds with such small donor−acceptor separations.

Most remarkably the fluorescence lifetime of **1C** is longer in polar media, while in less polar solvents such as diethyl ether and benzene it is shorter. In cyclohexane the lifetime of **1C** is again longer. Intuitively it is expected that, since the CT state of **1Si** is systematically situated at lower energies, charge recombination in **1Si** is faster and hence its fluorescence lifetimes will be shorter. The situation becomes more clear when the radiative decay rates, defined by $k_{rad} = \Phi_{fl}/\tau_{fl}$, are taken into consideration (Table 6); in a given solvent the decay of the CT state of **1C** is faster than that of **1Si**. The still remaining marked solvent dependence of the radiative rates of both compounds strongly suggests that locally excited (LE) states are involved in the decay process, *via* intensity borrowing.[60−62] The involvement of LE states can qualitatively be understood by the fact that owing to the small donor−acceptor separation and hence small excited state dipole moments the solvent stabilization on the CT states of **1Si** and **1C** is relatively small (eq 3). The CT states are thus lying close to the LE states, promoting their mutual electronic coupling.

When LE states are involved in the radiative decay process the decay rate depends, in addition to the electronic coupling between the ground and CT state *V*, on the coupling between the LE and CT state *V** and the transition dipole moment μ_{le} of the local excitation of energy E_{LE}:[60]

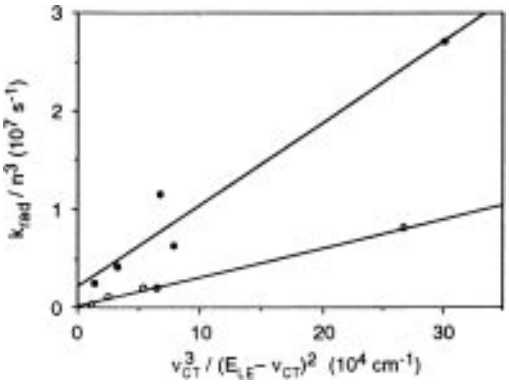

Figure 6. Linear fits of k_{rad}/n^3 *vs* $\nu_{CT}^3/(E_{LE} - \nu_{CT})^2$ for **1Si** (open circles) and **1C** (filled circles). Fitting results are $y = (2.11 \times 10^5) + 29.51x$, $r = 0.998$ for **1Si** and $y = (2.08 \times 10^6) + 83.3x$, $r = 0.973$ for **1C**.

$$k_{rad} = \frac{64\pi^4 n^3}{3h}[(V\Delta\mu)^2\nu_{CT} + 2VV^*(\Delta\mu\cdot\mu_{LE})\nu_{CT}^2/(E_{LE} - \nu_{CT}) + (V^*\mu_{LE})^2\nu_{CT}^3/(E_{LE} - \nu_{CT})^2] \quad (5)$$

In eq 5 $\Delta\mu = \mu_e - \mu_g$ and the couplings between states are defined by $V = \langle D^{\bullet+}\sigma A^{\bullet-}|\hat{H}|D\sigma A\rangle$ and $V^* = \langle D^{\bullet+}\sigma A^{\bullet-}|\hat{H}|D^*\sigma A\rangle$. When the mixing of the CT state with the LE state dominates the decay process only the last term of eq 5 has to be taken into account, leading to

$$k_{rad} = \frac{64\pi^4 n^3}{3h}(V^*\mu_{LE})^2\nu_{CT}^3/(E_{LE} - \nu_{CT})^2 \quad (6)$$

This relationship predicts a linear relationship between k_{rad}/n^3 and $\nu_{CT}^3/(E_{LE} - \nu_{CT})^2$. Taking $E_{LE} = 37\,300$ cm^{-1} for **1Si** and $E_{LE} = 39\,100$ cm^{-1} for **1C** (the maxima of the ^1L_a bands, the nearest lying bands for which mixing with the CT state is symmetry allowed) indeed linear relations are found between these quantities (Figure 6). The linear fit for **1Si** is excellent, whereas that for **1C** is somewhat less satisfactory. Nevertheless, the coupling between the CT and LE states in both **1Si** and **1C** is convincingly demonstrated. The coupling parameter *V** can be obtained from the slope of the fits, provided that μ_{LE} is known. This transition dipole moment is obtained using

$$|\mu_{LE}|^2 = \frac{3he^2 f_{LE}}{8\pi^2 m_e \omega_{LE}} \quad (7)$$

with ω_{LE} the absorption frequency (s^{-1}) and $3he^2/8\pi^2 m_e = 7.095 \times 10^{-43}$ m^2 s^{-1} C^2. The oscillator strength of the local excitation f_{le} is given by

$$f_{LE} = (4.32 \times 10^{-9})\epsilon_{max}\Delta\nu_{1/2} \quad (8)$$

where $\Delta\nu_{1/2}$ is the band width at half height in cm^{-1}. The values of interest for **3Si** are $\Delta\nu_{1/2} = 2890$ cm^{-1}, $f_{LE} = 0.35$, and $\mu_{LE} = 4.4$ D. For **3C** they are $\Delta\nu_{1/2} = 3540$ cm^{-1}, $f_{LE} = 0.29$, and $\mu_{LE} = 4.0$ D. It follows that $V^* = 2190$ cm^{-1} for **1Si** and $V^* = 4080$ cm^{-1} for **1C**. The CT state of **1C** is thus stronger coupled to the LE state than is the case for **1Si**.

According to eq 6 the fits in Figure 6 should have an intercept of zero. This applies for **1Si** but not for **1C**. Consequently, lower order terms in eq 5 including *V* should be taken into consideration to describe the behavior of **1C**, whereas they can be neglected for **1Si**. It can thus be concluded that the electronic coupling between the CT and ground state *V* is larger for the carbon compound as well.[63]

(59) Hermant, R. M.; Bakker, N. A. C.; Scherer, T.; Krijnen, B.; Verhoeven, J. W. *J. Am. Chem. Soc.* **1990**, *112*, 1214−1221.
(60) Bixon, M.; Jortner, J.; Verhoeven, J. W. *J. Am. Chem. Soc.* **1994**, *116*, 7349−7355.
(61) Gould, I. R.; Young, R. H.; Mueller, L. J.; Albrecht, A. C.; Farid, S. *J. Am. Chem. Soc.* **1994**, *116*, 3147−3148.
(62) Verhoeven, J. W.; Scherer, T.; Wegewijs, B.; Hermant, R. M.; Jortner, J.; Bixon, M.; Depaemelaere, S.; De Schryver, F. C. *Recl. Trav. Chim. Pays-Bas* **1995**, *114*, 443−448.

The foregoing analysis is valid on the conditions that the degree of admixture of the LE state into the CT state g^*, given by

$$g^* = [V^*/(E_{LE} - \nu_{CT})]^2 \quad (9)$$

is small: $g^* < 0.1$ and $V^* \ll E_{LE} - \nu_{CT}$. These conditions are fulfilled quite well with the exception of **1C** in cyclohexane ($g^* = 0.19$, Table 6). It must however be realized that the obtained V^* values are strongly associated with the magnitude of the local excitation transition dipole moment μ_{LE} as the product $V^*\mu_{LE}$ is obtained from the slopes of the fits. It has been shown[62] that application of μ_{LE} of only the first local transition often leads to an underestimated value. The effective magnitude of μ_{LE}, which incorporates contributions of several local excitations, may be a factor of 3 to 4 larger. The consequence is that V^* (and hence g*) is the same factor smaller, and in retrospect the applied analysis is justified.

The g^* data show that the admixture of the LE into the CT state decreases with increasing solvent polarity. The consequence is that CT state lifetimes are short in nonpolar solvents because decay *via* the short lived LE state is prominent. The shorter lifetimes of **1C** in nonpolar media are related to the larger extent of mixing of the CT and LE states in this compound. In polar solvents the lifetimes are more an intrinsic property of the CT states themselves. In these solvents the lifetimes of **1Si** are shorter since its CT state is situated at lower energies. Furthermore the small g^* value in all solvents indicates that CT state dipole moments are hardly affected by the admixture of LE states, and can be considered to be virtually independent of the solvent polarity.

Solid State Structures and Properties of 1Si and 1C. The molecular structures of **1Si**[26] and **1C** have been determined by single-crystal X-ray diffraction (Figure 7, Tables 7−9). Both compounds crystallize in the same space group (*Pnma*), are located on a crystallographic mirror plane, and possess similar structures. In both compounds the geometry around the bridging atom is essentially tetrahedral, with bond angles ranging from 107.00(6)° to 112.11(8)° in **1Si** and from 107.7(2)° to 111.2(2) in **1C** (Table 9). The geometry around the dimethylamino nitrogen atoms is nearly planar, indicating that these nitrogen atoms are to a large extent sp^2 hybridized. In **1C** the sum of bond angles around N(2) is 356.3(4)°, and the C(13)−N(2)−C(12)−C(11) dihedral angle is 12.7(5)°. In the silane the corresponding parameters are 357.09(18)° and 10.8(2)°. The sp^2 hybridization of nitrogen atoms, allowing maximal overlap between their lone pairs and the benzene π-systems, is usual for *N*,*N*-dimethylanilines.[64]

Interestingly, an increased quinoid character of the ground state of the (dimethylamino)phenyl group in **1Si** can be distinguished. This quinoid contribution can be expressed by a parameter *Q*,[66] which is in this case

$$Q = 1/2(d_{9-10} + d_{11-12}) - d_{10-11} \quad (10)$$

where *d* denotes the distance between the indicated carbon atoms. *Q* is zero for D_{6h} benzene, and 0.138 for a perfect quinoid structure with a single bond length of 1.455 Å and a double bond length of 1.317 Å.[66] For the (dimethylamino)-phenyl ring in **1Si** *Q* is 0.018(2) Å, while it is 0.000(5) Å in **1C**. The latter result is somewhat surprising, since a small quinoid contribution is expected to be present in dimethylanilines. We attribute the apparent absence of quinoid contributions in **1C** to the unexpected short C(9)−C(10) distance of 1.383(3) Å. Even though the increased quinoid character in **1Si** is indicative of a (ground state) CT interaction between the dimethylamino group and the silicon bridge, reflecting the latter's electron accepting properties. The presence of the CT interaction in **1Si** is also manifested by the shorter N(2)−C(12) distance (1.377(2) Å in **1Si**, 1.393(5) Å in **1C**) and the larger difference between the M−C(9) bond length (1.8576(19) Å in

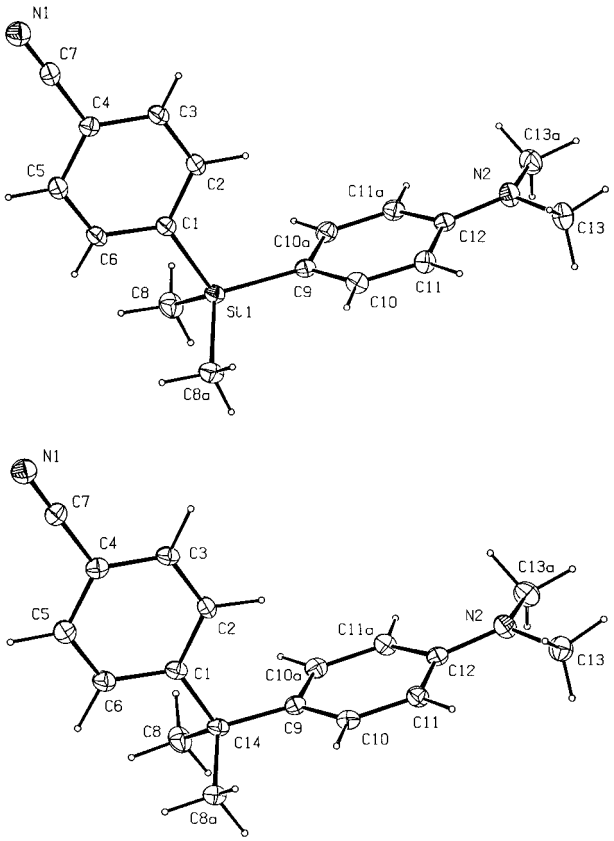

Figure 7. ORTEP[65] (30% probability level) drawing of **1Si** (top) and **1C** (bottom).

Table 7. Crystallographic Data for **1Si** and **1C**

	1Si	**1C**
formula	$C_{17}H_{20}N_2Si$	$C_{18}H_{20}N_2$
mol wt	280.44	264.37
cryst system	orthorhombic	orthorhombic
space group	*Pnma* (No. 62)	*Pnma* (No. 62)
a, Å	11.7053(5)	11.4551(12)
b, Å	9.7903(10)	9.6451(12)
c, Å	13.6840(14)	13.1648(13)
V, Å^3	1568.2(2)	1454.5(3)
D_{calc}, g·cm^{-3}	1.188	1.207
Z	4	4
F(000)	600	568
μ[Mo Kα], cm^{-1}	1.4	0.7
cryst size, mm	0.5 × 0.4 × 0.4	0.4 × 0.2 × 0.2
T, K	150	150
final R^a	0.042 [1582$F_o > 4\sigma(F_o)$]	0.066 [799$F_o > 4\sigma(F_o)$]
final $wR2^b$	0.098	0.138
goodness of fit	1.06	0.99

$^a R = \sum||F_o| - |F_c||/\sum|F_o|$. $^b wR2 = [\sum[w(F_o^2 - F_c^2)^2]/\sum[w(F_o^2)^2]]^{1/2}$.

(63) Very recently fitting procedures for a quantitative evaluation of *V* have been developed (ref 62). Unfortunately they cannot be reliably applied here because of the limited number of available data points. Application of the procedures, however, seems to establish that the coupling between ground and CT state is larger for **1C**.

(64) Maier, J. P.; Turner, D. W. *J. Chem. Soc., Faraday Trans. 2* **1973**, *69*, 521−531.

(65) Spek, A. L. *Acta Crystallogr.* **1990**, *A46*, C34.

(66) Bertolasi, V.; Feretti, V.; Gilli, P.; de Benedetti, P. G. *J. Chem. Soc., Perkin Trans. 2* **1993**, 213−219.

Table 8. Bond Lengths (Å) in **1Si** and **1C** with esd's in Parentheses

bond	**1Si**	**1C**	bond	**1Si**	**1C**
N(1)−C(7)	1.122(3)	1.140(6)	C(4)−C(5)	1.396(3)	1.400(6)
N(2)−C(12)	1.377(2)	1.393(5)	C(4)−C(7)	1.462(3)	1.453(6)
N(2)−C(13)	1.448(2)	1.448(4)	C(5)−C(6)	1.384(3)	1.380(7)
C(1)−C(2)	1.402(3)	1.391(6)	C(8)−M	1.8611(19)	1.541(4)
C(1)−C(6)	1.398(3)	1.407(6)	C(9)−C(10)	1.3973(16)	1.383(3)
C(1)−M[a]	1.8872(18)	1.542(5)	C(9)−M	1.8576(19)	1.531(6)
C(2)−C(3)	1.379(3)	1.387(6)	C(10)−C(11)	1.3835(19)	1.390(4)
C(3)−C(4)	1.393(3)	1.381(6)	C(11)−C(12)	1.4051(16)	1.397(3)

[a] M: Si(1) in **1Si**, C(14) in **1C**.

1Si, 1.531(6) Å in **1C**) and the M−C(1) bond length (1.8872(18) Å in **1Si**, 1.542(5) Å in **1C**). Thus, the difference between these bond lengths is 0.030(3) Å for **1Si** and 0.011(8) for **1C**. Quinoid contributions in the cyanophenyl moieties of **1Si** (Q = 0.016(7) Å) and **1C** (Q = 0.011(14) Å) are of similar magnitude.

The most remarkable feature in the X-ray structures is the orthogonality of the donor and acceptor chromophores, with the cyanophenyl moieties lying in the plane bisecting the (dimethylamino)phenyl groups. Concerning **1Si** this geometry differs markedly from the X-ray structure of dimethylbis(tetrathiafulvanelyl)silane, which possesses a butterfly conformation (see Figure 9) with an angle of 88.92° between the normals to the tetrathiafulvanelyl planes.[48] Other 2,2-diphenylpropanes in which the phenyl groups are arranged orthogonally are known, but scarce.[67] It would be expected that attractive forces between the donor and acceptor moieties force **1Si** and **1C** in particular into a spatial arrangement in which a through-space donor−acceptor interaction is possible. Apparently these forces are weak. It is not so that the orthogonal geometry around the bridging atoms prevents steric repulsions between the methyl carbon atoms and phenyl protons positioned ortho to the bridge. A close contact of 2.57(3) Å between C(8)a and H(10) is found in the structure of **1C**. This distance, which is 0.33 Å less than the sum of contact radii of carbon and hydrogen (2.90 Å), has also been reported to be present in another conformation of the 2,2-diphenylpropane skeleton.[68] The steric crowding leads to a nonequivalence of the C(1)−C(14)−C(8) and C(8)−C(14)−C(9) bond angles.[68] Although the C(8)a−H(10) distance in **1Si**, 2.95(3) Å, is larger a similar difference between the bond angles is found. The occurrence of the orthogonal geometry in **1C** is even more surprising as it leads to the extreme short C(9)−H(2) distance of 2.40(4) Å. The respective distance in **1Si** is 2.86(2) Å, close to the sum of contact radii. In the crystal packing structures of **1Si** and **1C**, donor and acceptor sites on neighboring molecules are also oriented orthogonally, leading to an edge to face packing motif.[69]

The orthogonality of donor and acceptor orbitals in **1Si** and **1C** renders it interesting to investigate their solid state UV spectra, which are depicted in Figure 8. The spectra are compared with those of the (solid) *bis*substituted reference compounds **9Si**, **9C**, **10Si**, and **10C** since compounds **3Si**, **3C**, **5Si**, and **5C** were liquids. Inspection of data in Table 1 reveals that these *bis*substituted compounds exhibit their UV maxima at the same positions as the monosubstituted compounds. The solid state UV spectra of the donor−acceptor compounds are in close agreement with their solution analogues; similar maxima

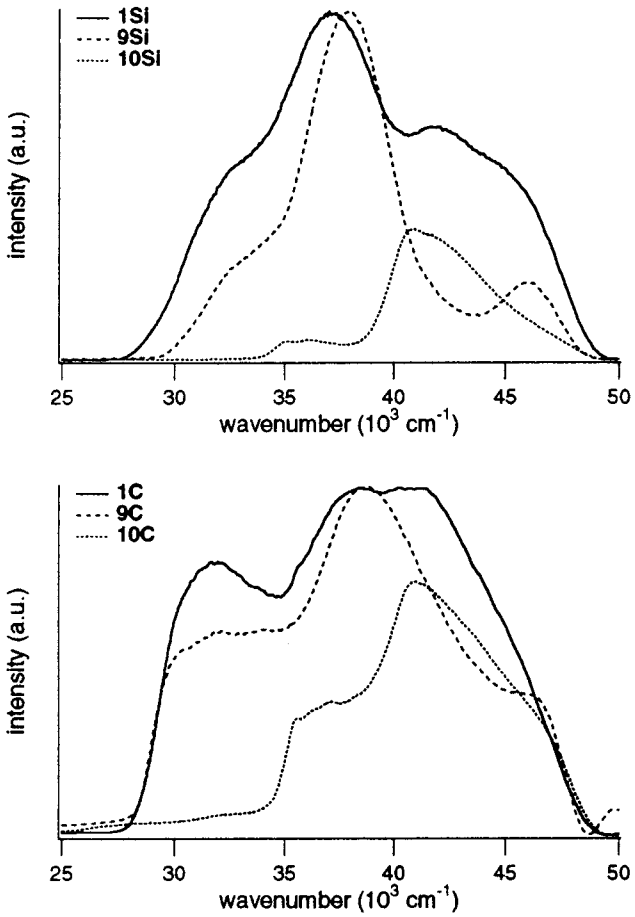

Figure 8. Solid state UV spectra (KBr matrix) of **1Si** and **1C** and their *bis*substituted reference chromophores.[29]

are found.[70] Although a quantitative comparison is not feasible it is evident that even in the solid state UV spectra of **1Si** and **1C** are more than a superposition of reference chromophore bands. In both cases an additional (CT) absorption at approximately 31 000 cm^{-1} is distinguishable. The orthogonality of donor and acceptor orbitals at both the molecular and supramolecular level excludes both an intramolecular through-bond and an intermolecular through-space ground state interaction. Although an NMR study on 4-substituted diphenyldimethylsilanes and 2,2-diphenylpropanes provided evidence that substituent effects extend beyond the bridging atoms,[29] this transmission of substituent effects, indicative of a ground state interaction, is operative *via* σ-orbitals (bond polarization mechanism), which prevents an interaction with orbitals of π-symmetry. An intramolecular through-space donor−acceptor interaction in the solid state structures of **1Si** and **1C** is however feasible. All π-type orbitals of the cyanophenyl moiety are antisymmetric with respect to the crystallographic mirror plane, and can overlap with (dimethylamino)phenyl orbitals such as the SHOMO and the LUMO (Figure 2) which are antisymmetric with respect to this plane as well. In particular p-type AO's of atom C(2), which is nearest to the dimethylamino ring, are involved. The overlap must however be very small, suggesting once more that intensity borrowing contributes significantly to the CT transitions.

Discussion and Conclusions

The apparently conflicting situation has arisen that the electronic interactions of the bridge with the donor and acceptor

(67) Cambridge Structural Database, Version 5.10, October 1995. Allen, F. H.; Kennard, O. *Chem. Design Automation News* **1993**, *8*, 31−37.
(68) Perez, S.; Scaringe, R. P. *Macromolecules* **1987**, *20*, 68−77.
(69) Jorgensen, W. L.; Severance, D. L. *J. Am. Chem. Soc.* **1990**, *112*, 4768−4774.

(70) The intensities of the ^1L_a bands appear to be relatively small, which is attributed to poor reflectance of samples at wavenumbers higher than 42 000 cm^{-1}.

Table 9. Selected Bond Angles (deg) in **1Si** and **1C** with esd's in Parentheses

bond angle[a]	**1Si**	**1C**	bond angle	**1Si**	**1C**
C(12)−N(2)−C(13)	119.69(9)	119.3(2)	C(10)−C(9)−M	122.25(8)	121.94(18)
C(13)−N(2)−C(13)a	117.71(14)	117.7(3)	N(2)−C(12)−C(11)	121.50(8)	121.58(17)
C(2)−C(1)−M[b]	123.47(14)	122.9(3)	C(1)−M−C(8)	107.00(6)	107.7(2)
C(6)−C(1)−M	119.51(14)	119.4(3)	C(1)−M−C(9)	110.18(8)	111.2(3)
C(3)−C(4)−C(7)	119.54(18)	120.3(4)	C(8)−M−C(9)	110.22(6)	110.6(2)
C(5)−C(4)−C(7)	120.10(18)	119.4(4)	C(8)−M−C(8)a	112.11(8)	108.8(3)
N(1)−C(7)−C(4)	177.9(2)	179.7(5)			

[a] Suffix a denotes symmetry operation x, $^1/_2-y$, z for **1Si** and x, $^3/_2-y$, z for **1C**. [b] M: Si(1) in **1Si**, C(14) in **1C**.

Figure 9. Through-space overlap of p atomic orbitals of diphenyldimethylsilanes and 2,2-diphenylpropanes in a butterfly conformation.

moieties are more pronounced for **1Si**, whereas the electronic coupling of the CT state with both the LE and the ground state is larger for **1C**. The larger couplings in **1C** can best be explained by assuming that a through-space mechanism is operative. Although the X-ray structures show that the donor and acceptor moieties are orthogonally positioned, this molecular conformation is in equilibrium with other forms in solution. Other conformations involved in the equilibrium in these types of compounds, *i.e.* monoatomically bridged diphenyls, are the twist (propeller) and butterfly forms.[66,71,72] Especially in the latter conformation spatial overlap between p atomic orbitals on phenyl carbon atoms adjacent to the bridge is possible (Figure 9).[47,73] Since the C−C bond length is shorter than the Si−C bond length (Table 8), the spatial overlap is larger for the carbon-bridged compounds, which explains the stronger interstate couplings. This way of reasoning is supported by the supposed larger rate of intersystem crossing *via* exciton coupling in the diphenylpropanes. Another contemplation which suggests the involvement of a through-space mechanism is that, even when in solution the orthogonality of the donors and acceptors exists, the geometry of excited states can be quite different.

In summary, the nature of the monoatomic bridges under investigation has a profound effect on the CT process. Thermodynamically charge transfer is more favorable for the $SiMe_2$ bridge, which can be traced back to a lowering of the cyanophenyl reduction potential by the silicon bridge. On the other hand, the electronic coupling of the CT state with both the LE state and the ground state is larger for the CMe_2 bridge, which is primarily associated to its smaller size. The photophysics of **1Si** and **1C**, in which the donor−acceptor distance is very short, are dominated by intensity borrowing, which has been demonstrated by both the solution and solid state electronic spectra and the radiative decay behavior.

Furthermore, we have shown that an intramolecular CT absorption occurs in a donor−acceptor substituted monosilane, while other workers could not detect such an absorption.[23,24] The CT absorption is however likely to be based on a through-space interaction, by which it is unfortunately not possible to evaluate the intrinsic ability of silicon, as compared to carbon, to transmit electronic effects.

The intensity of the CT absorption is too small to expect interesting second-order nonlinear optical responses for donor−acceptor substituted diphenyldimethylsilanes, despite the quite large excited state dipole moments. It has indeed been recognized previously that the first hyperpolarizability of donor−acceptor substituted diphenyldimethylsilanes can be described by a vector summation of the hyperpolarizabilities of the Dσ and σA chromophores.[23] The same should be true for the donor−acceptor substituted 2,2-diphenylpropanes.

Experimental Section

General. Reactions involving organolithium reagents and/or silyl chlorides were conducted in a nitrogen atmosphere using standard Schlenk techniques. Starting materials and reagents were obtained from commercial sources and used as received. Acetone, DMF, DMSO, and methanol were stored on 4 Å or 3 Å molecular sieves prior to use. Other solvents generally were distilled before use; diethyl ether was distilled from sodium−benzophenone. Column chromatography was performed on Merck kieselgel 60 silica (230−400 ASTM).

NMR spectra were obtained on a Bruker AC 300 apparatus, operating at 300 MHz for ^{1}H, 75 MHz for ^{13}C, and 60 MHz for ^{29}Si NMR. ^{29}Si NMR spectra were recorded with a proton decoupled inverse gated pulse sequence; samples contained chromium(III) acetylacetonate as relaxation reagent. Infrared spectra were recorded using a Perkin Elmer 283 infrared spectrometer. Solids were measured as KBr pellets and liquids between NaCl plates. GC-MS spectra were collected on a ATI Unicam Automass System 2 quadrupole mass spectrometer. Melting points were determined using a Mettler FP5/FP51 photoelectric apparatus. For gas chromatography a Varian 3700 chromatograph equipped with a DB5 capillary column was used. Elemental analyses were carried out at Kolbe Microanalytisches Laboratorium, Mülheim an der Ruhr, Germany.

Cyclic voltammetry measurements were performed with a Heka PG 287 potentiostat/galvanostat in acetonitrile (Janssen p.A. grade, freshly distilled from calcium hydride) containing 0.1 M tetrabutylammonium hexafluorophosphate (Fluka, electrochemical grade) as supporting electrolyte at scanning rates of 0.1 $V \cdot s^{-1}$. Redox potentials were determined relative to Ag/(0.1 M $AgNO_3$ in acetonitrile) and were referenced to SCE by regularly measuring the oxidation potential of the $FeCp/FeCp^{\bullet+}$ couple ($E_{1/2}$ *vs* SCE = 0.31 V[74]) in this system.

Solution UV spectra were measured using a Cary 1 spectrometer in spectrophotometric grade solvents (Janssen). Solid state UV spectra were collected with a Cary 5 UV−vis−NIR spectrophotometer using a Harrick praying mantis diffuse reflectance accessory on powdered dispersions (approximately 1% w/w) in KBr. Reflectance ordinates R were transformed into Kubelka-Munk units $F(R)$ by $F(R) = (1 - R)^2/2R$. Fluorescence spectra were obtained on a Spex Fluorolog instrument, equipped with a Spex 1680 double excitation monochromator, a Spex 1681 emission monochromator, and a Spex 1911F detector. Solvents (Janssen) generally were of spectrophotometric grade and dried on molecular sieves prior to use. Butyronitrile (Janssen, p.A.), di-*n*-butyl ether (Janssen, 99%), and di-*n*-pentyl ether (Aldrich, 99%) were distilled before use. Fluorescence emission spectra were corrected for the detector spectral response with the aid of a correction file provided by the manufacturer. Since this file does not cover the spectral range above 33300 cm^{-1}, fluorescence maxima in this region are uncorrected. Fluorescence quantum yields were determined relative to naphthalene ($\Phi_{fl} = 0.23$)[75] at an excitation wavelength of 265 nm. Solutions were degassed by purging with argon during 15 min. Fluorescence lifetimes were determined using a Lumonix EX700 XeCl excimer laser (308

(71) Bothorel, P. *Annu. Chim. (Paris)* **1959**, *13*, 669−712.
(72) Edlund, U.; Norström, Å. *Org. Magn. Reson.* **1977**, *9*, 196−202.
(73) Craenen, H. A. H.; Verhoeven, J. W.; de Boer, T. J. *Recl. Trav. Chim. Pays-Bas* **1972**, *91*, 405−416.
(74) Dachbach, J.; Blackwood, D.; Pons, J. W.; Pons, S. *J. Electroanal. Chem.* **1987**, *237*, 269−273.
(75) Eaton, D. F. *Pure Appl. Chem.* **1988**, *60*, 1107−1114.

nm, 8.4 ns fwhm) as excitation source, monitoring the fluorescence signal at a right angle by a RCA C-31025C photodiode *via* a Zeiss MQ II monochromator. The signal was fed into a Tektronix TDS 684A oscilloscope triggered by a photodiode that detects the laser pulse. Samples ($A < 0.2$ at 308 nm) were degassed by purging with argon. A description of the equipment and experimental details of the flash photolysis TRMC technique can be found elsewhere.[55,56]

Extended Hückel (EH) calculations were performed with the CACAO program[76,77] on PM3[78,79] optimized (precise option) geometries. Silicon d orbital parameters, not implemented in CACAO, were taken from the Forticon8 program.[80] Other parameters used in both programs are identical. All calculations were run on a 486/33 MHz personal computer.

X-ray Structure Determinations. Details of the structure determination of **1Si** have been reported elsewhere;[26] pertinent data have been included in Table 7. A colorless crystal of **1C** suitable for X-ray diffraction was glued to the tip of a Lindemann-glass capillary and transferred into the cold-nitrogen stream of an Enraf-Nonius CAD4-T diffractometer on rotating anode. Accurate unit-cell parameters and an orientation matrix were determined by least-squares fitting of the setting angles of 25 well-centered reflections (SET4[81]) in the range $11.40° < \theta < 14.05°$. The unit-cell parameters were checked for the presence of higher lattice symmetry.[82] Crystal data and some details on data collection are presented in Table 7. Reflection data were collected in ω scan mode with scan angle $\Delta\omega = 0.50 + 0.35 \tan\theta°$. Intensity data of 3869 reflections were collected in the range $1.55° < \theta < 27.50°$, 1768 of which are independent. Data were corrected for *Lp* effects and for a linear decay of 6% of the three periodically measured reference reflections ($\bar{2}$ 2 2, 2 2 2, 0 2 2) during 10 h of X-ray exposure time, but not for absorption. The structure was solved by automated direct methods (SHELXS86[83]). Refinement on F^2 was carried out by full-matrix least-squares techniques (SHELXL-93[84]); no observance criterion was applied during refinement. Hydrogen atoms were located on a difference Fourier map and their coordinates were included in the refinement. Non-hydrogen atoms were refined with anisotropic thermal parameters. The hydrogen atoms were refined with a fixed isotropic thermal parameter related to the value of the equivalent isotropic displacement parameter of their carrier atoms by a factor of 1.5 for the methyl hydrogen atoms and 1.2 for the other hydrogen atoms. In the final refinement cycles 141 parameters were optimized using the weighting scheme $w = [\sigma^2(F^2) + (0.0303P)^2]^{-1}$, with $P = (Max(F_o^2,0) + 2F_c^2)/3$. A final difference Fourier map showed no residual density outside -0.20 and 0.24 e·Å^{-3}. Positional parameters are included in the supporting information. Neutral atom scattering factors and anomalous dispersion corrections were taken from the *International Tables for Crystallography*.[85] Geometrical calculations and illustrations were performed with PLATON;[65] all calculations were performed on a DECstation 5000 cluster.

Syntheses. The preparation of the compounds **3Si**, **4Si**, **5Si**, **6Si**, **7Si**, and **8Si** has been reported previously.[29] The preparation and characterization of synthetic intermediates **13Si**, 2-(4-bromophenyl)-2-propanol, **13C**, **14**, **15**, **16**, **17**, **18**, **19**, **20**, **12C**, and **21** is described in the supporting information. 4-*tert*-Butyl-*N*,*N*-dimethylaniline (**6C**) was purchased from Aldrich and used as received.

(4-Bromophenyl)chlorodimethylsilane (11). A solution of 4-bromophenyllithium[86] (250 mmol) in 250 mL of diethyl ether was added to a solution of dichlorodimethylsilane (92 mL, 670 mmol) in 75 mL of diethyl ether at such a rate that the mixture refluxed gently. A white solid formed immediately. After finishing the addition the mixture was refluxed for an additional 2 h and stirred overnight at room temperature. The etheral solution was decanted under nitrogen and subsequently volatile components were distilled off at atmospheric pressure (35−80 °C). The residue was fractionally distilled under reduced pressure (0.2 mmHg). The fraction boiling at 92−96 °C proved to be **11**. Yield 24.40 g (98 mmol, 40%) of a colorless liquid. Purity 85% by GC. ^{1}H NMR ($CDCl_3$): δ 7.57 and 7.51 (AA′BB′, 2 × 2H, Ar-H), 0.71 (s, 6H, SiMe). GC-MS: *m*/*e* 248 ($M^{\bullet+}$).

(4-Bromophenyl)(4′-(dimethylamino0phenyl)dimethylsilane (12Si). A solution of 4-bromo-*N*,*N*-dimethylaniline (6.70 g, 33.5 mmol) in 50 mL of diethyl ether was added dropwise to finely cut lithium pieces (0.64 g, 92.2 mmol) in 20 mL of diethyl ether. The mixture was stirred overnight at room temperature; GC showed that at that time the starting compound was not present anymore. The turbid solution was filtered over quartz wool into a dropping funnel and added to a solution of **11** (8.01 g, purity 85%, 27.3 mmol) in 20 mL of diethyl ether, after which the mixture was refluxed overnight. Water (25 mL) was added cautiously, and the layers were separated. Subsequently the organic layer was washed with 3 × 25 mL of a 10% ammonium chloride solution, dried on magnesium sulfate, and filtered. After concentration under reduced pressure a purple liquid was obtained, which solidified on standing. **12Si** (7.32 g, 21.9 mmol, 80%) was obtained in the form of white crystals after flash chromatography (silica, chloroform) and recrystallization from pentane. Mp 58 °C. ^{1}H NMR ($CDCl_3$): δ 7.50 and 7.41 (AA′BB′, 2 × 2H, Ar-H), 7.39 and 6.77 (2 × AA′XX′, 2H, Ar-H), 2.99 (s, 6H, NMe), 0.53 (s, 6H, SiMe). ^{13}C NMR ($CDCl_3$): δ 151.2, 138.4, 135.8, 135.3, 130.8, 123.7, 122.2, 112.0 (all aromatic C), 40.2 (NMe), −2.2 (SiMe). ^{29}Si NMR ($CDCl_3$): δ −8.4. IR (KBr): 2815 (NMe_2), 1250, 835−800 (SiMe), 1115 (Si-Ar) cm^{-1}.

(4-Cyanophenyl)(4′-(dimethylamino)phenyl)dimethylsilane (1Si). In a nitrogen atmosphere, a mixture of **12Si** (2.52 g, 7.54 mmol), copper(I) cyanide (0.82 g, 9.15 mmol), and 5 mL of DMF was refluxed for 5 h. The cooled brownish mixture was then poured into 100 mL of 25% ammonia. After passing air through this suspension for 3.5 h under vigorous stirring, it was extracted with 3 × 30 mL of chloroform. The combined organic layers were concentrated to a volume of *ca.* 10 mL, and 75 mL of hexane was added. This solution was washed with water (3 × 50 mL), dried on magnesium sulfate, filtered, and evaporated under reduced pressure. The resulting brownish solid was purified by flash chromatography (eluent chloroform) and recrystallization from methanol. Yield 1.58 g (56.3 mmol, 75%) of block shaped crystals with a greenish glance. Mp 128 °C. Anal. Calcd for $C_{17}H_{20}N_2Si$: C, 72.81; H, 7.19; N, 9.99; Si, 10.01. Found: C, 72.66; H, 7.25; N, 9.95; Si, 9.88. ^{1}H NMR ($CDCl_3$): δ 7.66 and 7.61 (AA′BB′, 2 × 2H, Ar-H), 7.42 and 6.79 (AA′XX′, 2 × 2H, Ar-H), 3.01 (s, 6H, NMe), 0.58 (s, 6H, SiMe). ^{13}C NMR ($CDCl_3$): δ 151.4, 146.7, 135.3, 134.6, 130.9, 121.0, 112.4, 112.0 (all aromatic C), 119.2 (CN), 40.1 (NMe), −2.4 (SiMe). ^{29}Si NMR ($CDCl_3$): δ −7.9. IR (KBr): 2820 (NMe_2), 2230 (CN), 1260, 835−800 (SiMe), 1115 (Si-Ar) cm^{-1}.

(4-Cyanophenyl)(4′-methoxyphenyl)dimethylsilane (2Si). This compound was prepared as described for its dimethylamino analogue **1Si**. It was purified by column chromatography (eluent chloroform) and obtained as white crystals upon trituration with methanol. Yield 76%. Mp 41 °C. Anal. Calcd for $C_{16}H_{17}NOSi$: C, 71.87; H, 6.41; N, 5.24; Si, 10.50. Found: C, 70.21; H, 6.50; N, 5.11; Si, 10.15. ^{1}H NMR ($CDCl_3$): δ 7.60 (AA′BB′, 4H, Ar-H), 7.42 and 6.94 (AA′XX′, 2H, Ar-H), 3.83 (s, 3H, OMe), 0.56 (s, 6H, SiMe). ^{13}C NMR ($CDCl_3$): δ 160.9, 145.9, 135.6, 134.6, 131.0, 127.2, 113.9, 112.6 (all aromatic C), 119.0 (CN), 55.1 (OMe), −2.5 (SiMe). ^{29}Si NMR ($CDCl_3$): δ −7.4. IR (KBr): 2830, 1250, 1030 (Ar-O-Me), 2235 (CN), 1255, 840−800 (SiMe), 1115 (Si-Ar) cm^{-1}.

2-(4-Methoxyphenyl)-2-phenylpropane (4C). In a 1-necked flask 2-phenylpropanol (3.78 g, 27.7 mmol) and 85% phosphoric acid (3 mL, 43.8 mmol) were mixed. To the white suspension was added anisole (3.00 g, 27.7 mmol) and the mixture was stirred overnight at 90 °C. After addition of 25 mL of diethyl ether the solution was washed three times with 15 mL of water, dried on magnesium sulfate, and filtered. The diethyl ether was removed in a rotary evaporator and the mixture was kugelrohr distilled, collecting the fraction boiling in the

(76) Mealli, C.; Proserpio, D. M. *CACAO*, Version 3.0: Florence, 1992.
(77) Mealli, C.; Proserpio, D. M. *J. Chem. Educ.* **1990**, *67*, 399−402.
(78) Stewart, J. J. P. *J. Comp. Chem.* **1989**, *10*, 209−220.
(79) Stewart, J. J. P., *MOPAC*, Version 6.0; Serena Software: Bloomington, 1990; QCPE Program 504.
(80) Howell, J.; Rossi, A.; Wallace, D.; Haraki, K.; Hoffmann, R., *Forticon8*, QCPE QCMP011.
(81) de Boer, J. L.; Duisenberg, A. J. M. *Acta Crystallogr.* **1984**, *A40*, C410.
(82) Spek, A. L. *J. Appl. Crystallogr.* **1988**, *21*, 578.
(83) Sheldrick, G. M., SHELXS86 Program for crystal structure determination, University of Göttingen, Germany, 1986.
(84) Sheldrick, G. M., SHELXL93 Program for crystal structure refinement, University of Göttingen, Germany, 1993.
(85) *International Tables for Crystallography*; Wilson, A. J. C., Ed.; Kluwer Academic: Dordrecht, 1992; Vol. C.
(86) Eisch, J. J. *Non-Transition Metal Compounds*; *Organometallic Synthesis. Vol. 2;* Academic: New York, 1981; p 93.

range 120−135 °C (0.1 mmHg). This fraction was separated into its components with column chromatography. The first component (2.04 g, 8.63 mmol, 31%) was eluted with hexane and was identified as 2,4-diphenyl-4-methyl-1-pentene by ^{1}H NMR, IR, and GC-MS (2,4-diphenyl-4-methyl-1-pentene is one of the dimers of the reaction intermediate α-methylstyrene[87−89]). The second component was isolated after elution with ethyl acetate−hexane 1:1 (v/v) and proved to be **4C**. Yield 1.32 g (5.83 mmol, 21%) of a colorless oil. Anal. Calcd for $C_{16}H_{18}O$: C, 84.91; H, 8.02. Found: C, 84.82; H, 7.96. ^{1}H NMR ($CDCl_3$): δ 7.37 (m, 4H, Ar-H), 7.24 (m, 1H, Ar-H), 7.22 and 6.90 (AA′XX′, 2 × 2H, Ar-H), 3.85 (s, 3H, OMe), 1.75 (s, 6H, CMe). ^{13}C NMR ($CDCl_3$): δ 157.4, 150.8, 142.7, 127.9, 127.7, 126.6, 125.4, 113.2 (all aromatic C), 54.9 (OMe), 42.2 (*C*Me), 30.8 (C*Me*). IR (NaCl): 2830, 1250, 1030 (Ar-O-Me) cm^{-1}.

2-(4-Cyanophenyl)-2-(4′-methoxyphenyl)propane (2C). This compound was prepared from **13C** (1.81 g, 5.93 mmol) and copper(I) cyanide (0.63 g, 7.08 mmol) as described for **1Si**. The crude product was purified by column chromatography (eluent chloroform−hexane 2:1 (v/v)) to give 1.07 g (4.26 mmol, 72%) of a colorless liquid. Anal. Calcd for $C_{17}H_{17}NO$: C, 81.24; H, 6.82; N, 5.57; O, 6.37. Found: C, 81.31; H, 6.78; N, 5.49; O, 6.45. ^{1}H NMR ($CDCl_3$): δ 7.58 and 7.37 (AA′BB′, 2 × 2H, Ar-H), 7.15 and 6.87 (AA′XX′, 2 × 2H, Ar-H), 3.82 (s, 3H, OMe), 1.71 (s, 6H, CMe). ^{13}C NMR ($CDCl_3$): δ 157.9, 156.6, 141.2, 132.0, 127.7, 127.6, 113.6, 109.4 (all aromatic C), 119.1 (CN), 54.9 (OMe), 42.8 (*C*Me), 30.5 (C*Me*). IR (NaCl): 2830, 1250, 1040 (Ar-O-Me), 2240 (CN) cm^{-1}.

2,2-Bis(4-cyanophenyl)propane (10C). Synthesis of this compound from **17** was performed following the same procedure as employed for the other cyanides. After purification by flash chromatography (eluent chloroform) and recrystallization from methanol **10C** was isolated in the form of white crystals. Yield 71%. Mp 143 °C. Anal. Calcd for $C_{17}H_{14}N_2$: C, 82.90; H, 5.73; N, 11.37. Found: C, 82.76; H, 5.71; N, 11.31. ^{1}H NMR ($CDCl_3$): δ 7.57 and 7.30 (AA′BB′, 2 × 4H, Ar-H), 1.69 (s, 6H, CMe). ^{13}C NMR ($CDCl_3$): δ 154.5, 132.1, 127.5, 110.2 (all aromatic C), 118.6 (CN), 43.9 (*C*Me), 30.0 (C*Me*). IR (KBr): 2220 (CN) cm^{-1}.

2-(4-(Dimethylamino)phenyl)-2-phenylpropane (3C). A solution of amine **18** (0.49 g, 2.32 mmol) and methyl iodide (1.2 mL, 19.3 mmol) in 10 mL of ethanol was refluxed overnight in the presence of potassium carbonate (1.60 g, 11.6 mmol). After cooling to room temperature solids were filtered off and washed thoroughly with water. The filtrate, in which another crop of solid had precipitated, was filtered again, and the residue was washed as well. The combined residues were dried in a vacuum desiccator over potassium hydroxide. The quaternary amine salt (0.79 g) was subsequently boiled for 5 min in 5 mL of freshly distilled ethanolamine. Water (10 mL) was added, and the resulting brown liquid precipitate was isolated by extraction with 3 × 10 mL of methylene chloride, drying on calcium chloride, filtering, and evaporation of the solvent. Pure **3C** was obtained as a light tanned solid after column chromatography with chloroform as eluent. Yield 0.34 g (1.42 mmol, 61% with respect to amine **18**). Mp 36 °C. Anal. Calcd for $C_{17}H_{21}N$: C, 85.31; H, 8.84; N, 5.85. Found: C, 85.21; H, 8.81; N, 5.79. ^{1}H NMR ($CDCl_3$): δ 7.36 (m, 4H, Ar-H), 7.23 (m, 1H, Ar-H), 7.21 and 6.76 (AA′XX′, 2H, Ar-H), 3.00 (s, 6H, NMe), 1.76 (s, 6H, CMe). ^{13}C NMR ($CDCl_3$): δ 151.3, 148.5, 138.7, 127.8, 127.4, 126.7, 125.3, 112.2 (all aromatic C), 42.0 (*C*Me), 40.6 (NMe), 30.8 (C*Me*). IR (KBr): 2830 (NMe_2) cm^{-1}.

2,2-Bis(4-(dimethylamino)phenyl)propane (9C). Bisamine **19** was methylated using the same method as employed for the methylation of **18**. Yield 61% of light pink crystals after recrystallization from methanol. Mp 82 °C. Anal. Calcd for $C_{19}H_{26}N_2$: C, 80.80; H, 9.28; N, 9.92. Found: C, 80.68; H, 9.22; N, 9.86. ^{1}H NMR ($CDCl_3$): δ 7.14 and 6.68 (AA′XX′, 2 × 4H, Ar-H), 2.95 (s, 12H, NMe_2), 1.64 (s, 6H, CMe). ^{13}C NMR ($CDCl_3$): δ 148.5, 139.5, 127.4, 112.3 (all aromatic C), 41.1 (*C*Me), 40.7 (NMe), 31.0 (C*Me*). IR (KBr): 2810 (NMe_2) cm^{-1}.

2-(4-Cyanophenyl)-2-(4′-(dimethylamino)phenyl)propane (1C). This compound was prepared as described for **1Si**. Purification was carried out with column chromatography (eluent chloroform) and recrystallization from methanol. Yield 0.41 g (1.55 mmol, 30%) of crystals with a greenish glance. Mp 136 °C. Anal. Calcd for $C_{17}H_{14}N_2$: C, 81.78; H, 7.63; N, 10.59. Found: C, 81.66; H, 7.58; N, 10.52. ^{1}H NMR ($CDCl_3$): δ 7.56 and 7.37 (AA′BB′, 2 × 2H, Ar-H), 7.09 and 6.71 (AA′XX′, 2 × 2H, Ar-H), 2.95 (s, 6H, NMe), 1.69 (s, 6H, CMe). ^{13}C NMR ($CDCl_3$): δ 157.2, 148.9, 136.9, 131.8, 127.6, 127.4, 112.4, 109.3 (all aromatic C), 119.2 (CN), 42.6 (*C*Me), 40.6 (NMe), 30.5 (C*Me*). IR (KBr): 2820 (NMe_2), 2230 (CN) cm^{-1}.

2-(4-Cyanophenyl)-2-phenylpropane (5C). 2-(4-Bromophenyl)-2-phenylpropane (**21**, 0.54 g, 1.96 mmol) was converted into the corresponding cyanide following the approach as described for **1Si**. After purification by column chromatography (eluent chloroform) a colorless oil (0.17 g, 0.76 mmol, 41%) was obtained. Anal. Calcd for $C_{16}H_{15}N$: C, 86.84; H, 6.83; N, 6.33. Found: C, 86.94; H, 6.83; N, 6.36. ^{1}H NMR ($CDCl_3$): δ 7.56 and 7.35 (AA′BB′, 2 × 2H, Ar-H), 7.32−7.21 (m, 5H, Ar-H), 1.72 (s, 6H, CMe). ^{13}C NMR ($CDCl_3$): δ 156.2, 148.9, 131.8, 128.2, 127.5, 126.5, 126.1, 109.4 (all aromatic C), 119.0 (CN), 43.3 (*C*Me), 30.2 (C*Me*). IR (NaCl): 2230 (CN) cm^{-1}.

4-*tert*-Butylbenzonitrile (8C). This compound was synthesized from 4-bromo-*tert*-butylbenzene as described for the synthesis of **1Si**. After distillation (boiling range 67−69 °C, 0.1 mmHg) a colorless liquid was obtained in 71% yield. ^{1}H NMR ($CDCl_3$): δ 7.57 and 7.46 (AA′BB′, 2 × 2H, Ar-H), 1.31 (s, 9H, CMe). ^{13}C NMR ($CDCl_3$): δ 156.6, 131.9, 126.2, 109.3 (all aromatic C), 119.1 (CN), 35.3 (*C*Me), 30.9 (C*Me*). IR (NaCl): 2230 (CN), 1370 (CMe_3) cm^{-1}.

4-*tert*-Butylanisole (7C). Potassium carbonate (27.20 g, 196.8 mmol) was added in one portion to a solution of 4-*tert*-butylphenol (9.95 g, 66.24 mmol) in 100 mL of DMSO. After the mixture was stirred for 50 min methyl iodide (5 mL, 80.3 mmol) was added dropwise, keeping the temperature at 18 °C by cooling with an ice-bath. Subsequently the mixture was stirred 1 h at 45 °C and overnight at room temperature. Since GC analysis showed the presence of some starting material another 3 mL of iodomethane (48 mmol) were added, and stirring was continued for 2 h at 50 °C. Water (500 mL) was then added and the mixture was extracted with 3 × 50 mL of methylene chloride. The combined organic layers were concentrated under diminished pressure, after which the residual yellow liquid was dissolved in 60 mL of hexane and washed with 50 mL of 5% potassium hydroxide solution and 3 × 50 mL of water. After drying on magnesium sulfate, filtering, and evaporation of the solvent the residual liquid was vacuum distilled over a vigreux column (bp 58 °C at 0.1 mmHg). Yield 7.83 g (47.7 mmol, 72%) of a colorless liquid. ^{1}H NMR ($CDCl_3$): δ 7.38 and 6.92 (AA′XX′, 2 × 2H, Ar-H), 3.85 (OMe), 1.38 (s, 9H, CMe). ^{13}C NMR ($CDCl_3$): δ 157.4, 143.4, 126.2, 113.4 (all aromatic C), 55.2 (OMe), 34.1 (*C*Me), 31.6 (C*Me*). IR (NaCl): 2820, 1250, 1040 (Ar-O-Me), 1370 (CMe_3) cm^{-1}.

Acknowledgment. This work was supported in part (A.L.S) by the Netherlands Foundation of Chemical Research (SON) with financial aid from the Netherlands Organization for Scientific Research (NWO).

Supporting Information Available: Preparation and characterization of synthetic intermediates (**13Si**, 2-(4-bromophenyl)-2-propanol, **13C**, **14**, **15**, **16**, **17**, **18**, **19**, **20**, **12C** and **21**) and further details of the structure determination, including atomic coordinates, bond lengths and angles and thermal parameters for **1C** (Tables S1-7) (13 pages). See any current masthead page for ordering and Internet access instructions.

JA960546E

(87) Welsh, L. H.; Drake, N. L. *J. Am. Chem. Soc.* **1938**, *60*, 59−62.
(88) Kawakami, Y.; Toyoshima, N.; Yamashita, Y. *Chem. Lett.* **1980**, 13−16.
(89) Higashimura, T.; Nishii, H. *J. Polym. Sci., Polym. Chem. Ed.* **1977**, *15*, 329−339.